ADVANCED CONTROL OF AMMONIA REACTOR USING BLOCK-ORIENTED MODELS

A DISSERTATION

Submitted in partial fulfillment of the requirements for the award of the degree of

MASTER OF TECHNOLOGY

in

CHEMICAL ENGINEERING

(With Specialization in Industrial Safety and Hazard Management)

By

SURESH PALUKURI

DEPARTMENT OF CHEMICAL ENGINEERING
INDIAN INSTITUTE OF TECHNOLOGY ROORKEE
ROORKEE-247 667 (INDIA)

JUNE, 2006

CANDIDATE'S DECLARATION

I hereby declare that the work, which is being presented in this project report, entitled **"Advanced Process Control of Ammonia reactor using Block-Oriented Models"**, submitted in partial fulfillment of the requirements for award of the degree of **Master of Technology** in **Chemical Engineering** with the specialization in **Industrial Safety and Hazards Management (ISHM)**, is an authentic record of my own work carried out under the supervision of **Dr. Nidhi Bhandari**, Assistant Professor, Department of Chemical Engineering, Indian Institute of Technology Roorkee, Roorkee.

Date: 29/06/2006

Place: Roorkee

(Suresh Palukuri)

CERTIFICATE

This is to certify that the above statement made by the candidate is correct to the best of my knowledge.

Dr. Nidhi Bhandari

Assistant Professor

Department Of Chemical Engineering

Indian Institute of Technology Roorkee

Uttaranchal-247667

ACKNOWLEDGEMENTS

I wish to express my deep sense of gratitude and sincere thanks to my guide **Dr.** Nidhi Bhandari, Department of Chemical Engineering, IIT Roorkee, for being helpful and a great source of inspiration. Her keen interest and constant encouragement gave me the confidence to complete my work. I wish to extend my sincere thanks for the excellent guidance and suggestions for the successful completion of my work.

I am also thankful to all my friends for their continuous support and help during different stages of my project work.

(Suresh Palukuri)

ABSTRACT

Ammonia is one of the most important chemicals produced as it enjoys the wide use in the manufacture of fertilizers. Hence, modeling and simulation of ammonia manufacturing process has received considerable attention among the process industries way from 1960s.

Most chemical processes are inherently nonlinear. In recent years, nonlinear process identification has received more attention in both research institutions and industries. One way to specify model structure is to combine linear dynamic models with static (memoryless) nonlinear functions. These kind of nonlinear models are called **Block-Oriented models.** Mostly, unless specified otherwise, all studied nonlinear models will have a block-oriented structure: different building blocks will be assembled in specific configurations and studied.

Commonly used block-oriented models are Hammerstein model, Weiner model and their combinations. A Hammerstein model has nonlinear block followed by a linear model and a Weiner model has nonlinear model with a linear dynamic block followed by a static nonlinear function.

In this work, ammonia reactor model is taken and simplified by using some assumptions and approximations. Then its state-space model is developed. Using the state-space model, the reactor temperature is controlled.

CONTENTS

LIST OF FIGURES

LIST OF TABLES

NOMENCLATURE

SYMBOLS AND NOTATIONS

u(t)	input signal at the time t	
y(t)	output signal at the time t	
v, w	unmeasurable time domain signals between two blocks	
C_{pc}	specific heat of catalyst	kcal/kg mole ^{0}K
C_{pi}	specific heat of ***i*** th component	
	(i = 1 for hydrogen, 2 for nitrogen	kcal/kgmole ^{0}K
	3 for ammonia and 4 for inerts)	
$\overline{C}_{p0}$	average heat capacity of feed gas	kcal/kg mole ^{0}K
F	molar flow rate of feed	kg moles/hr
F_j	flow in the ***j*** th branch	
	(j= 1 for heat exchanger shell	kg moles/hr
	2 for heat exchanger bypass	
	3 for direct bypass)	
FF_i	molar flowrate of ***i*** th component in the feed gas	kg moles/hr
S	heat transfer area in catalyst bed	m^2
S'	heat transfer area in heat exchanger	m^2
s_2	total surface available for heat transfer	m^2
	between tube wall-catalyst section	
T_B	reference temperature	25 °C
T_C	catalyst temperature	°C
T_F	feed temperature	°C
T_T	temperature in the lube of catalyst portion	°C

T'_T	temperature in the tub-e of heat exchanger	°C
T'_s	temperature in the shell of heat-exchanger	°C
U	overall heat transfer coefficient in catalyst bed	kcal/hr m² °C
U'	overall heat transfer coefficient in heat exchanger	kcal/hr m² °C
V	volume of the catalyst bed	m³
W	weight of the catalyst	kg
Y	yield of ammonia	kg moles/hr
$d(t)$	disturbance vector	-
h_2	average heat transfer coefficient from wall to catalyst	kcal/hr m² °C
l'	length of the heat exchanger	m
r	reaction rate	$\frac{\text{kgmole}NH_3}{\text{hr.m}^3\text{catalyst}}$
$x(t)$	state vector	-
y	mole fraction of ammonia	-
α	normalized distance, catalyst portion	-
α'	normalized distance, heat exchanger	-
β	ratio of heat exchanger bypass to heat exchanger flow	-
γ	ratio of direct bypass flow to heat exchanger bypass	-
δ	ratio of heat exchanger flow to feed flow	-
ΔC	decrease in specific heat due to formation of one mole of ammonia	kcal/kg mole °K
ΔH_0	enthalpy of formation of ammonia at 298 °K	kcal/kg mole
θ	nondimensional unit of time $\left(\theta = \frac{h_2 s_2}{WC_{pc}} t\right)$	-
v_S	velocity of gas mixture in the shell side of heat exchanger	m/sec
v_T	velocity of the gas mixture in the tube of heat exchanger	m/sec

$t_c(i), i = 1,5$	incremental catalyst temperature at the ***i*** th location	^{0}C
$t'_t(i), i = 1,2$	incremental tube temperature in heat exchanger at ***i*** th location,	^{0}C
$t'_s(i), i = 0,1$	incremental shell temperature in heat exchanger at ***i*** th location,	^{0}C
u_i	incremental flow rates (manipulated variables)	kg moles/hr
	$i = 1$ main stream flow in heat exchanger	
	$i = 2$ heat exchanger bypass flow	
	$i = 3$ direct bypass flow	
$u(t)$	control vector	-
t_f	incremental feed temperature	^{0}C
y_0	incremental feed composition	-

Superscripts

* inlet condition

Transfer functions of **LTI** systems are written in upper case letters:

R transfer function of the input linear system of a Wiener or a Wiener-Hammerstein system

S transfer function of the linear system inside a Hammerstein or Hammerstein- Wiener system or of the output linear system of a Wiener-Hammerstein system

ABBREVIATIONS

LTI Linear Time Variant

FRF Frequency Response Function

NARMAX Nonlinear Auto-Regressive Moving Average with eXogenous inputs

RLDS Related Linear Dynamic System. The RLDS is the best linear approximation of a nonlinear system.

ODE ordinary differential equations

PDE partial differential equations

CHAPTER - 1

INTRODUCTION

Building complex systems demands that the composing subsystems are well known. Modeling and identification offer a solution for this request: given a set of measurements, mathematical equations are constructed that allow predicting or simulating the performance of a device before building it. This is an essential cost saver, both in production materials that are not wasted and in time that is not spent to build a prototype that a simulation would have shown to fail. This time, that is not lost, is translated into a reduced time to market. Also, these models can give insight in the working of the device and help to understand which modifications are necessary to obtain a desired behavior.

If sufficient prior knowledge and physical insight is present, a so-called *white-box model* can be built. This means that by looking to the physics of the device, a series of equations describing the device is proposed. These equations contain unknown parameters that are estimated by fitting the model to the measurements. However, as the size of the system grows, a second force comes into play: the complexity that can be handled is limited. At the other extreme are *black-box models*: no prior knowledge is used and a model structure is proposed. Then the element of the set of models that best explains the measurements is retained as the model. The set of models is usually a family of systems described by unknown parameters, so that choosing the aforementioned element is done by minimizing some cost function with respect to the parameters. Black-box models describe the behavior of a system.

1.1 IMPORTANCE OF NON-LINEAR MODELS

Linear models have been used for a long time and their identification is a mature science. However linear modeling is not always sufficient: each model is only an approximation of reality and many systems are in fact nonlinear. For many inputs, linear approximations are valid and very useful, but as the input range is increased, the nonlinear effects become so important that they can't be ignored anymore.

Nonlinear behavior comes in all shapes and colors. Mostly, nonlinear models are an approximation to reality.

OPEN LOOP NONLINEAR SYSTEMS

If the output of a system is a nonlinear function of its input, but not of its output, the nonlinear system is called an open loop nonlinear system. A discrete time open loop nonlinear system could be written as [3]

$$y(t) = F(u(t), u(t-1),.....) \qquad \text{..... (1.1)}$$

where u(t) input signal at the time t

y(t) output signal at the time t

F nonlinear function

CLOSED LOOP NONLINEAR SYSTEMS

In contrast to the open loop nonlinear systems, closed loop nonlinear systems include the output in the nonlinear input output relation [3]

$$y(t) = F(u(t), u(t-1),\ldots\ldots, y(t-1), y(t-2),\ldots\ldots) \qquad \ldots\ldots\ldots\ldots \textbf{(1.2)}$$

APPROXIMATING NONLINEAR SYSTEMS

The field of nonlinear systems, as discussed above, is huge. Therefore, it is very difficult or sometimes impossible to propose a model structure for all nonlinear systems at once.

Thus, depending on the system, different approaches exist to propose models for nonlinear dynamic systems. Some of these approaches will be presented shortly here, focusing on the class of systems that can be modeled. Since no model structure can cover all possible nonlinear systems, approximations will be introduced. However, these approximations (and their approximation properties) depend on the input signal and the approximation criterion.

DIFFERENT SYSTEMS, DIFFERENT MODELS

The different models and their approximation properties for nonlinear systems are introduced. Table 1.1 is a summary of different models and their approximation properties for nonlinear systems.

Table 1.1: Convergence properties of different nonlinear model classes. **[3]**

Model	Notes
Wiener models	• Mean square convergence to Wiener systems with saturations and discontinuities. Derivatives of signals converge for band limited input. • Uniform convergence for Volterra systems (Wiener systems with analytic nonlinearities) for a limited system dependent input range (similar to Taylor expansion, derivatives of the system converge, too) • Uniform convergence for fading memory systems (Wiener systems with continuous discontinuities) over a user chosen input range. Derivatives of signals converge for band limited input.
Non recurrent Neural Networks	Uniform convergence for continuous open loop nonlinear systems. No result was found in the literature about the convergence of the derivatives.
Recurrent Neural Network	Uniform convergence for continuous closed loop nonlinear systems for bounded $u(t)$ and $x(t)$ for a finite time. No result was found in the literature about the convergence of the derivatives.
Bilinear models	Uniform convergence for continuous closed loop nonlinear systems for bounded $u(t)$ and $x(t)$ for a finite time. No result was found in the literature about the convergence of the derivatives.
NARMAX models	Uniform convergence for continuous closed loop nonlinear systems for bounded $u(t)$ and $x(t)$. No result was found in the literature about the convergence of the derivatives.

1.2 DEVELOPMENT OF DYNAMIC MODELS

A brief description of deriving the dynamic models of the chemical processes is given here. Dynamic models are nothing but unsteady-state models derived from physical and chemical principles. A dynamic model can be used to characterize the transient behavior of a process for a wide variety of conditions. Development of a suitable process model can be a crucial step to success.

TYPES OF MODELS

Models can be classified based on how they are obtained:

a) ***Theoretical models*** are developed using the principles of chemistry, physics, and biology.
b) ***Empirical models*** are obtained by fitting experimental data.
c) ***Semi-empirical models*** are a combination of the models in categories (a) and (b); the numerical values of one or more of the parameters in a theoretical model are calculated from experimental data.

Theoretical models offer two very important advantages: they provide physical insight into process behavior, and they are applicable over wide ranges of conditions. However, there are disadvantages associated with theoretical models. They tend to be expensive and time-consuming to develop. In addition, theoretical models of complex processes typically include some model parameters that are not readily available, such as reaction rate coefficients, physical properties, or heat transfer coefficients.

Although empirical models are easier to develop than theoretical models, they have a serious disadvantage: empirical models typically do not extrapolate well. More specifically, empirical models should be used with caution for operating conditions that were not included in the experimental data used to fit the model. The range of the data is typically quite small compared to the full range of process operating conditions.

Semi-empirical models have three inherent advantages: (i) they incorporate theoretical knowledge, (ii) they can be extrapolated over a wider range of operating conditions than empirical models, and (iii) that require less development effort than

theoretical models. Consequently, semi-empirical models are widely used in industry.

Dynamic models of chemical processes consist of ordinary differential equations (ODE) and/or partial differential equations (PDE), plus related algebraic equations.

DEGREES OF FREEDOM ANALYSIS

To simulate the process, we must first ensure that its model equations (differential and algebraic) constitute a solvable set of relations. In other words, the output variables, typically the variables on the left side of the equations, can be solved in terms of the output variables. That is, the equations must have a unique solution. In order for a model to have a unique solution, the number of unknown variables must be equal the number of independent model equations. An equivalent statement is that all of the available *degrees of freedom* must be utilized. The number of degrees of freedom, NF, can be calculated from the following expression,

$$NF=NV-NE \qquad \text{..... (1.3)}$$

where NV is the total number of process variables and NE is the total number of independent equations.

A degrees of freedom analysis allows modeling problems to be classified according to the following categories:

a) NF=0: the process model is *exactly specified*. If NF=0, the number of equations is equal to the number of process variables and set of equations has a solution. (However, the solution may not be unique for a set of nonlinear equations).

b) NF>0: the process is *underspecified.* If NF>0, then NV>NE so there more process variables than equations. Consequently, the NE equations have an infinite number of solutions because NF process variables can be specified arbitrarily.

c) NF<0: the process model is *overspecified.* For NF<0, there are fewer process variables than equations, and consequently the set of equations has no solution.

Note that NF=0 is the only satisfactory case. If NF>0, then a sufficient number of input variables have not been assigned numerical values. If NF<0, then additional independent model equations must be developed in order for the model to have an exact solution.

SOLUTION OF DYNAMIC MODELS

Once a dynamic model has been developed, it can be solved for a variety of conditions that include changes in the input variables or variations in model parameters. The transient responses of the output variables are calculated by numerical integration of the model equations. A large number of numerical integration techniques are available. Most commonly used methods are Runge-Kutta (RK) fourth order method and Euler's method. Euler's method is generally not used because of two reasons. Firstly, the truncation error per step associated with this method is far larger than those associated with other, more advanced, methods (for a given value of **h**). Secondly, Euler's method is too prone to numerical instabilities. So the most commonly used method is the Runge-Kutta 4^{th} order method. It is used to integrate the above mentioned ODEs (Ordinary Differential Equations). Softwares are also readily available for integrating ordinary and partial differential equations. Most popular ones include MATLAB, Mathematica, ACSL, aspen Custom Modeler and Mathcad.

1.3 INTRODUCTION TO BLOCK-ORIENTED SYSTEMS

The aim of this introduction is first to limit the scope to a reasonable size. Additionally, some basic concepts will be introduced, along with the notations.

There are several advantages for using block-oriented models **[20]:**

- Low cost in identification test.
- Low cost in identification computation.
- It is easy to comprehend and to incorporate a priori process knowledge.
- They are easy to use in control.

Except where noted otherwise, all studied nonlinear models will have a block-oriented structure: different building blocks will be assembled in specific configurations and studied. These structures are widely used and the most common have a specific name.

Linear time invariant (LTI) systems

This section introduces briefly the Linear Time Invariant (**LTI**) systems. These systems have been used for a long time and their identification has been studied very thoroughly. The **LTI** systems, represented by **Fig 1.1** in all schematics, introduce the dynamic behavior that makes the systems "interesting".

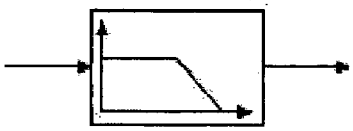

Fig. 1.1 Schematic representation of a linear system **[3]**

Definition 1.1 : A system is called LTI system if its input-output relation satisfies the following conditions:

- The system must be linear:

$$\left.\begin{array}{l} y_1(t) = H[u_1(t)] \\ \\ y_2(t) = H[u_2(t)] \end{array}\right\} \Rightarrow \forall \alpha_1, \alpha_2 : \alpha_1 y_1(t) + \alpha_2 y_2(t) = H[\alpha_1 u_1(t) + \alpha_2 u_2(t)] \quad \text{..... (1.3)}$$

- The system must be time invariant:

$$y(t) = H[u(t)] \Leftrightarrow y(t-\tau) = H[u(t-\tau)] \quad \text{..... (1.4)}$$

Static nonlinearities

The output of a static nonlinearity depends only on the present input value, but not on past (or future) inputs. These are the simplest nonlinear system imaginable. They are represented by a mathematical function which maps the input value at instant τ to the output value at the same instant. This concept is embodied in Figure 1.2 which symbolizes this nonlinear mapping function.

Fig. 1.2 Schematic representation of static nonlinear system **[3]**

Commonly used structures

The basic blocks can be assembled in series, yielding Hammerstein or Wiener systems when two blocks are used and Hammerstein-Wiener or Wiener-Hammerstein systems when three blocks are used. When identifying such model

structures, the difficulty lies in the fact that the signals between two blocks cannot be measured.

1.3.1 The Hammerstein system

As it can be seen in Figure 1.3, the input **u(t)** is first transferred through a static nonlinearity **f**. The unmeasured output **w(t)** of the static nonlinearity is eventually filtered by the linear system whose Frequency Response Function (FRF) is **S**.

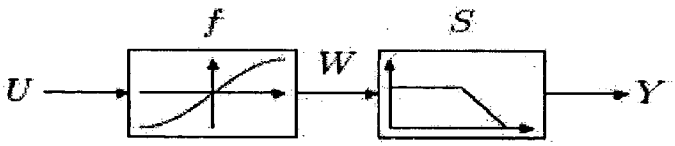

Fig. 1.3 A Hammerstein system

1.3.2 The Wiener system

They are grouped together because of their similarity illustrated by comparing Figure 1.3 with Figure 1.4. In the Wiener system, the input signal **u(t)** is filtered by the LTI system **R** first. The resulting signal **v(t)** is distorted afterwards by the static nonlinearity **f**. These are the same operations as for a Hammerstein system, but in a reversed order.

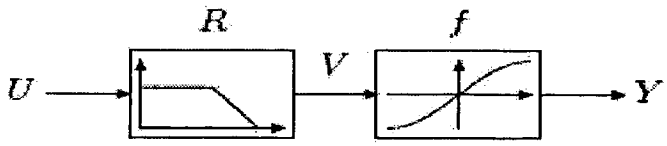

Fig 1.4 A Weiner system

1.3.3 The Hammerstein-Wiener system

A Hammerstein-Wiener system (Figure 1.5) is a combination of a Hammerstein system followed by a Wiener system: the linear part of both systems is concentrated into one linear block surrounded by two static nonlinear blocks. It presents an important difference with the Wiener or the Hammerstein system. This difference, along with an identification method for such systems is discussed in Chapter 5.

The first nonlinearity **f** could for example be the nonlinearity of an actuator in a plant, followed by the LTI behavior of this plant and its nonlinear characteristic **g**.

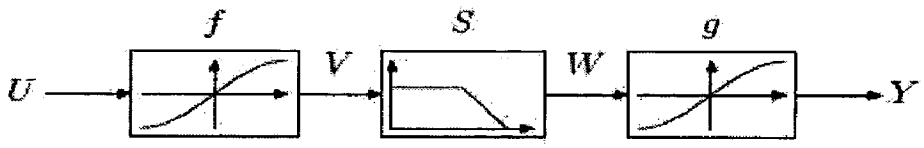

Fig. 1.5 A Hammerstein-Weiner system **[3]**

Identification of Hammerstein-Weiner model

Hammerstein-Wiener systems contain two nonlinear blocks and an Linear Time Invariant (LTI) block in cascade, connected as shown in Figure 1.5. They are particular because their RLDS is different from the underlying linear system under certain circumstances.

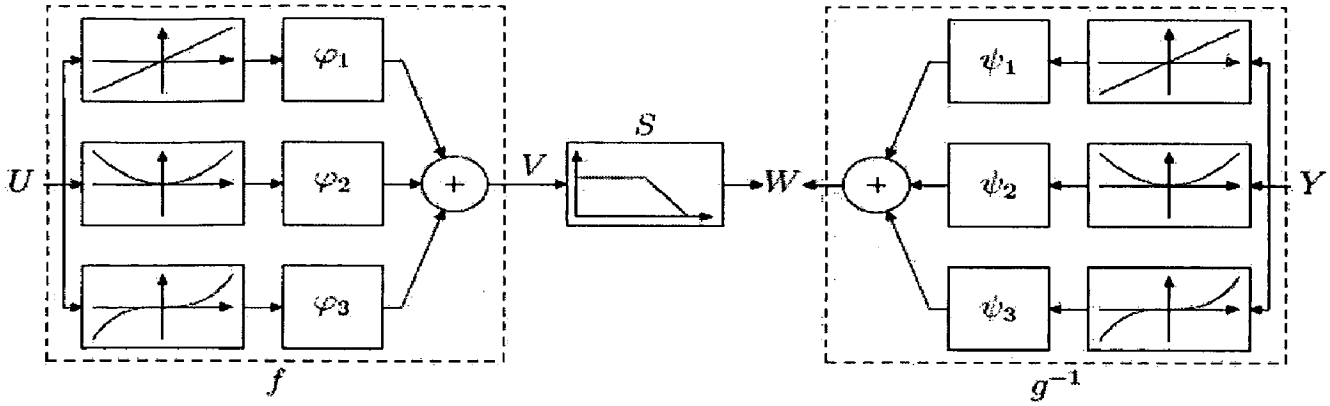

Fig. 1.6 Estimating W in two different ways. Pay attention to the direction of the arrows in the right part of the picture **[3]**.

The basic steps of the identification method of the RLDS of the Hammerstein-Wiener System will be given here.

Recall that in Figure 1.5, there is only one linear block, S. Taking inspiration from the identification procedure for Hammerstein systems, it is feasible to estimate the intermediate signal **W**, using the input data and the estimates of **f** and **S**. Looking at the estimation of Wiener systems, **W** could also be computed with the output data and the estimate of the inverse of **g**.

Roughly speaking, the identification of a Hammerstein-Wiener system could be attempted as follows (refer also to Figure 1.6):

1. Estimate the RLDS to estimate S.

2. Write **W** as a weighted sum of basic nonlinear contributions filtered by $\hat{S}$. These weights are the parameters that appear linearly in the estimate of **W** (because $\hat{S}$ is a linear operator).

3. Write **W** as a weighted sum of basis functions applied to **Y**.

4. Try and make both estimates of **W** equal (in a least squares sense). This yields an optimization problem that is easily solved, as the cost function is quadratic in the parameters (the weights from 2 and 3).

1.3.4 The Wiener-Hammerstein system

The system in this section that is the most difficult to estimate is the Wiener-Hammerstein system. This is because of the presence of the two LTI systems **R** and **S**. If there wasn't the static nonlinearity **f** it would even be impossible to separate those two LTI systems.

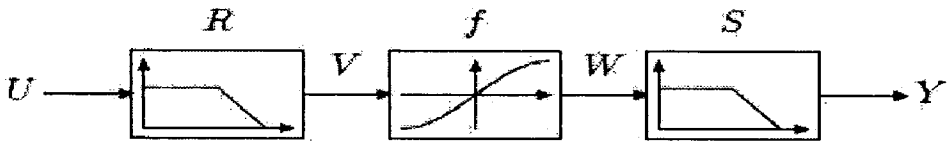

Fig. 1.7 A Weiner-Hammerstein system **[3]**

Identification method

Wiener-Hammerstein systems consist of two linear dynamic systems placed around a static nonlinearity. These models are difficult to identify due to the presence of two dynamic systems. Usually, a nonlinear estimation procedure is necessary to estimate the parameters of the different parts. This nonlinear estimation procedure needs good starting values to converge quickly and/or reliably to a global minimum.

Wiener-Hammerstein systems model the nonlinearity as a series of fundamental building blocks: linear dynamic systems and a static nonlinearity. It is plain to see that the static nonlinearity introduces the nonlinear behavior, while the linear dynamic systems allow to model the memory that might be present in the

system. Figure 1.7 shows the Wiener-Hammerstein structure as well as the symbols for the subsystems and the signal names used in this chapter.

However, identifying Wiener-Hammerstein systems is much more difficult than the previous systems.

The main objective of this work is to control the temperature of the ammonia reactor.

Chapter-2

LITERATURE REVIEW

Many chemical processes are non-linear in nature. Because of this reason, recent work on modeling methods shifted from linear models to nonlinear models.

This chapter consists of two sections.

1. *Multivariable control and block-oriented models*: it contains the different works done by different authors on various block-oriented models.
2. *Ammonia reactor*: it contains the discussion of some of the papers on ammonia reactor.

2.1. MULTIVARIABLE CONTROL AND BLOCK- ORIENTED MODELS DISCUSSION

Crama and **Schoukans (2004)** discussed about an iterative scheme for the identification of the Hammerstein-Weiner model, which is a block oriented model where a linear dynamic system is surrounded by two static nonlinearities at its input and output. It has been proven in the paper that in absence of modeling errors, the iterative procedure converges locally to the true values.

The main disadvantage of the in mentioned procedure is that it is only locally convergent to the true system. Since this method does not globally optimize the parameters of the model to minimize the cost function, its parameters should be used as initialization for a complex estimator optimizing all parameters at once.

Ender and **Filho (2000)** presented a new multivariable control strategy using neural networks. The proposed control strategy uses past and present process information to design the best controller, as well as to generate the new control actions. The neural networks can learn sufficiently accurate models and give good nonlinear control when model equations are not known or only partial state information is available. At each sampling time the controller is optimized, using the future error of the closed loop, generated by a neural model of the process. The process considered is the fixed bed catalytic rector for production of acetaldehyde by ethyl alcohol, which has a complex dynamic behavior. Though this reference not related to my work, I felt the technique used is very much efficient.

In my view, I think it is a worth writing a paragraph about neural networks. As mentioned before, neural networks learn almost accurate models and can give a good nonlinear control when model equations are not known or only partial state information is available. Neural network approach allows taking into account, in an elegant and adequate way process non-linearities as well as variable interactions. In process control applications neural networks can be incorporated in the control strategy in either direct of indirect methods. Multilayered feedforward neural networks represent a special form of connectionist model that performs a mapping from an input space to an output space. They consist of massively interconnected simple processing elements arranged in a layered structure; the strength of each connection is characterized by its assigned weight. The input neurons are connected to the output neurons through layers of hidden nodes. The processing of information I each neuron is performed through its activation function. When the hidden units have a nonlinear activation function the mapping is nonlinear. In the process control applications neural networks can be incorporated in the control strategy in either direct methods or indirect methods. In the direct methods, a

neural network is trained to represent the inverse dynamics of the system. In this case, given the current state of the dynamic system and the target state for the next sampling instant, the network is trained to produce the control action that drives the system to this target state. In the indirect method the neural network is trained with input-output data from the dynamic system to represent the forward dynamics; given the current state and current control action, the network learns to predict the next state of the system.

Nidhi Bhandari and **Rollins (2003)** proposes a multiple-input, multiple-output (MIMO) continuous-time modeling approach for the Wiener system that can accurately predict process behavior using only recent input data. The models are obtained from complete reliance on experimental data, and this work demonstrates the effectiveness of optimal statistical design of experiments (SDOE) to fully obtain Wiener models. This method is evaluated on a highly nonlinear continuous stirred tank reactor, and its performance is compared to conventional discrete-time Wiener modeling (DTM) using a pseudorandom sequence design (PRSD) and the same SDOE as the proposed method.

The first step in the proposed procedure is to select and run an experimental design that will contain adequate information to estimate all significant terms in the model. We have found that selecting the design points from a statistical design of experiment (SDOE) and running them as a series of sequential step tests will provide adequate ultimate response and dynamic response data (with an adequate sampling rate). Because sequential step tests are run from steady state to steady state (or approximately so), it is important to keep the number of step tests (i.e., design points) to a minimum. In this work, a new MIMO continuous time modeling method, W-BEST, was introduced for

Wiener-type processes, which have been almost exclusively modeled by discrete-time modeling methods.

Juan and **Enrique (2004)** proposed new noniterative algorithms for the identification of (multivariable) block-oriented nonlinear models consisting of the interconnection of linear time invariant systems and static nonlinearities are presented. The proposed algorithms are numerically robust, since they are based only on least squares estimation and singular value decomposition. Two different block-oriented nonlinear models are considered in this paper, viz., the Hammerstein model, and the Wiener model. Key in the derivation of the results is the use of basis functions for the representation of the linear and nonlinear parts of the models. The performance of the proposed identification algorithms is illustrated through simulation examples of two benchmark problems drawn from the process control literature, viz., a binary distillation column and a pH neutralization process.

Kenneth and **Ahmet (2003)** presented a case study of controlling a nonlinear polymerization reactor using functional expansion models. Functional expansion (FEx) models are a subclass of the general block-oriented model structure for nonlinear process systems. Controller design in this context uses the internal model control (IMC) paradigm. The primary advantage arises from the fact that inverting the nonlinear dynamic operator is avoided by taking advantage of the partitioned model inverse due to the special structure of FEx models. The robust stability and performance of the closed-loop system can be analyzed by expressing the FEx model as a linear uncertain system and using the structured singular value framework. By expressing nonlinearities in the closed-loop as linear systems with an associated uncertainty, the stability problem was converted to a linear stability problem.

2.2 AMMONIA REACTOR DISCUSSION

Patnaik,Viswanadham and **Sarma (1980)** developed a state space model of a tubular ammonia reactor which is the heart of an ammonia plant in a fertilizer complex. A ninth order model with three control inputs and two disturbance inputs is generated from the nonlinear distributed model using linearization and lumping approximations. The lumped model is chosen such that the steady state temperature at the exit of the catalyst bed computed from the simplified state space model is close enough to the one computed from the nonlinear steady state model. The model developed in this paper is very useful for the design of continuous/discrete versions of single variable/multivariable control algorithms. The number of discretization intervals for the purpose of lumping has been chosen after conducting a number of simulation experiments.

The proposed model consists of five partial differential equations and two algebraic equations with necessary boundary and initial conditions with respect to the space and time variables, respectively. After linearization and lumping approximations, and converting into state space form, it is simplified into nine ordinary differential equations.

In another paper in 1980, these same authors developed direct digital control strategies for the above mentioned ammonia reactor using quadratic regulator theory and compare the performance of the resultant control system with that under conventional PID regulators.

Brain, Baddour and **Eymery (1964)** simulated the dynamic behavior of a widely used type of ammonia synthesis reactor (The Tenessee Valley Authority Reactor) on a digital computer. The mathematical model, which retains the major

processes of transport and accumulation of enthalpy and matter, is solved by a series of finite difference analogs which proved to be highly efficient.

The transient behavior of the reactor is interpreted physically, and frequency responses and simplified transfer functions are proposed for operation within the linear range. The dynamic behavior of the reactor was shown to be linear for perturbations in the inlet temperature smaller than 5°C around the conditions of maximum production. Under these conditions the dynamic behavior of the reactor has been described successfully by approximate transfer functions. Despite its simplicity it was shown that the approximate transfer function describes the true dynamic behavior of the reactor in both the time and frequency domains. Therefore these functions should be useful for correlating dynamic data when they are available.

Baddour, Logeais, Brain, and **Eymery (1965)** developed a simple mathematical model of a T.V.A. ammonia synthesis reactor which approximates within 15 to 20% the temperature profiles and the ammonia production rates of an industrial reactor. With this model the effects of design and operating parameters upon reactor stability, ammonia production rate, and catalyst bed temperature profile have been studied. Using this simulation, the effects of space velocity, feed gas ammonia and inert contents, reactor heat conductance, and catalyst activity upon reactor stability, ammonia production rate, and catalyst bed temperature profile have been determined.

Chapter – 3

PROBLEM DESCRIPTION

3.1 REACTOR DESCRIPTION

Ammonia is formed according to the exothermic reaction,

$N_2 + 3H_2 \rightleftharpoons 2NH_3$.

The synthesis gas, which consists of hydrogen and nitrogen in the stoichiometric proportions of 3:1, is prepared in the reformer section of the plant. This gas mixture compressed to a pressure of 200-300 atmospheres enters the synthesis converter. **Fig 3.1** shows the schematic of the reactor under consideration. A simplified figure is given in **Fig 3.2.**

The converter consists of two parts:

(a) the catalyst bed section, and

(b) the heat-exchanger section.

The gases from the previous stage enter the reactor through the sheath between the converter shell and the cartridge housing the catalyst bed. To ensure stable conditions with maximum yield, it is necessary to heat the feed gases to a temperature of about 420°C before they enter the catalyst bed. This is economically achieved by preheating the feed gases first in the heat exchanger and subsequently in the tubes of the reacting section.

The inlet gaseous mixture is split into three separate streams:

(a) the main stream called the heat exchanger flow,

(b) the second stream called the heat exchanger bypass flow, and

(c) the third stream, known as the direct bypass flow.

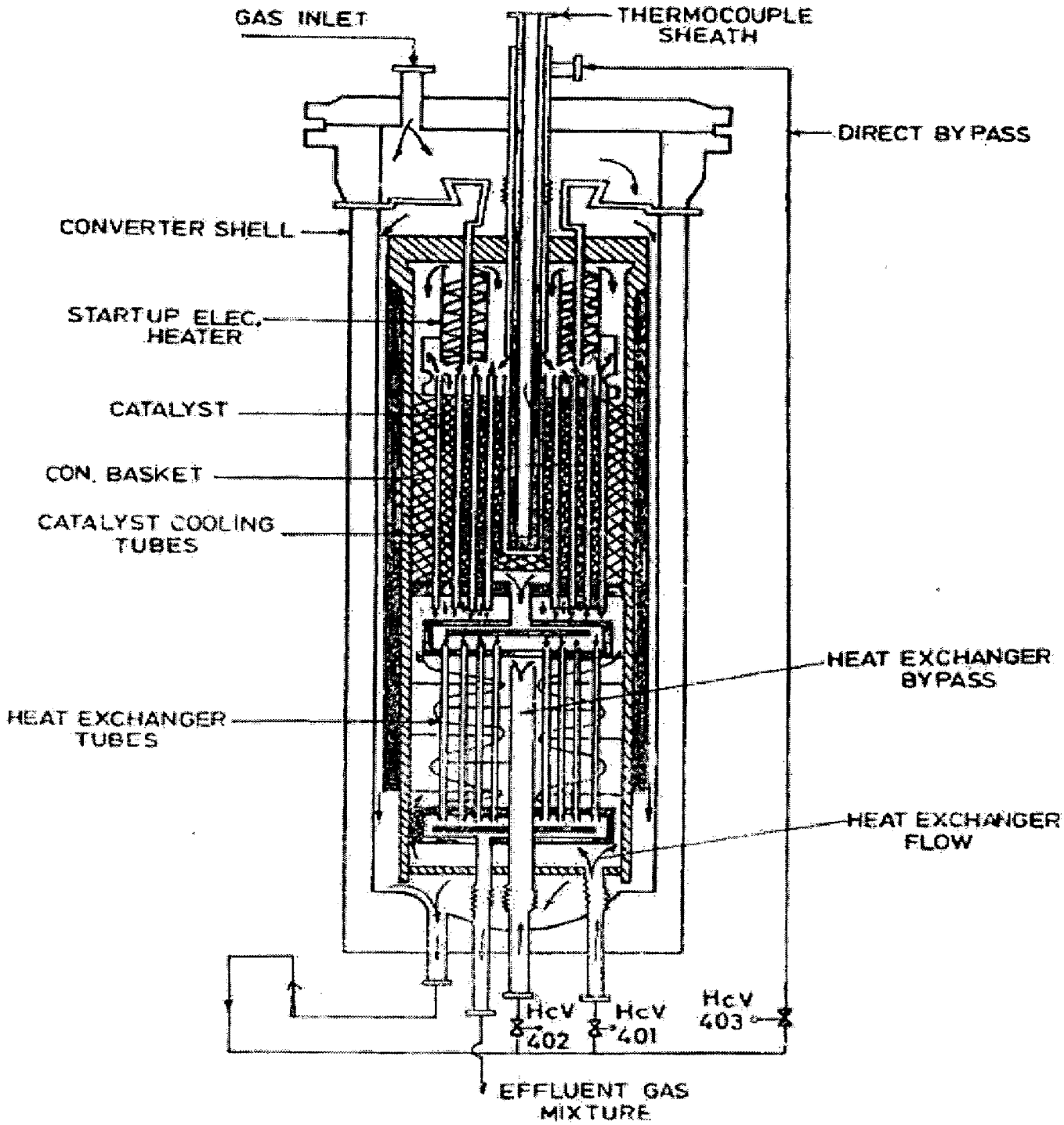

Fig. 3.1 Synthesis converter **[1].**

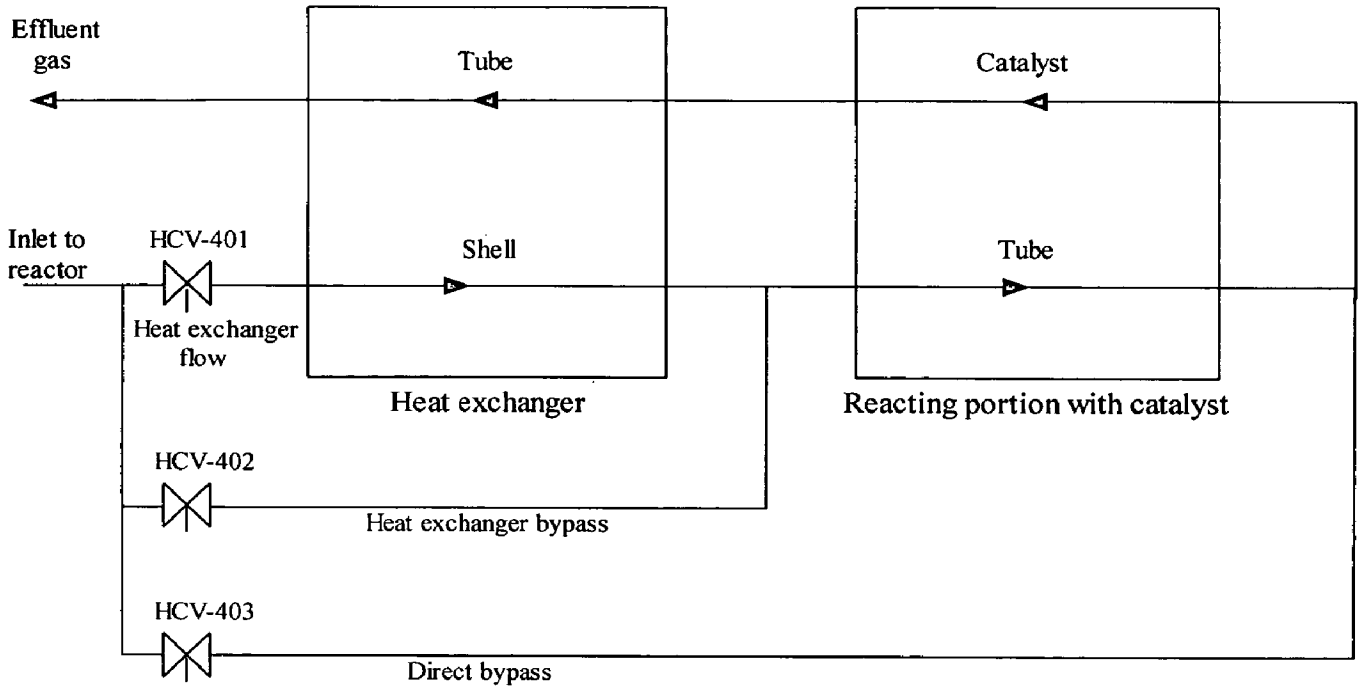

Fig. 3.2 Simplified schematic of ammonia synthesis converter [15].

The main stream enters the shell side of the heat exchanger via HCV-401. This gas stream is preheated by the hot gases flowing through the tubes. The second stream called the heat exchanger bypass flow, enters the reactor via HCV-402 and is mixed with the main stream leaving the shell side of the heat exchanger. The temperature of this mixture, which subsequently enters the tubes of the catalyst bed section, can be controlled by manipulating the heat exchange bypass flow. Due to heat transfer from the reacting gases flowing in the catalyst bed, the temperature of this gas mixture increases as it ascends the tube. The third stream known as the direct bypass flow enters the reactor via HCV-403 and mixes with the gas mixture (consisting of main stream and heat exchanger bypass) at the top of the converter. By controlling the direct bypass flow, the temperature of the feed gas entering the

converter is controlled. The feed gases now flow down the catalyst bed where the conversion of nitrogen and hydrogen to ammonia takes place. The outlet gases from the reactor enter the tubes of the heat exchanger and finally exit the converter.

The catalyst widely used in ammonia synthesis is reduced iron promoted with alumina and potassium oxide. The activity of the catalyst decays with age due to poisoning by gases such as CO_2, CO and sulphur compounds and also due to the high temperature to which it is subjected. Since catalyst softening occurs at high temperature, it is desirable to keep the maximum temperature in the reactor below 570^0C

The three flow rates can be varied using valves. Also adequate instrumentation exists to measure the process variables of interest. The temperatures at five points along the length of the reactor are measured using thermocouples. Also the inlet flows are measured using differential pressure type flow meter.

3.2 DATA FOR THE REACTOR

The data for this reactor is given in a paper by Patnaik et al. [14].

Table 3.1: Data of ammonia reactor

Number of tubes in catalyst portion	154
Volume of catalyst	3.2 m^3
Number of tubes in heat exchanger	1314
Inlet temperature to the reactor	41^0C
Outlet temperature from the reactor	232^0C

Heat exchanger flow rate	53000 m^3/hr
Direct bypass flow rate	3000 m^3/hr
Heat exchanger bypass rate	8000 m^3/hr
Analysis of gas at the inlet	H_2 – 65.5% N_2 – 22% NH_3 – 4.5% Inerts – 8%
Operating pressure	300 atm

The larger variation of temperature across the heat exchanger warrants the calculation of these below parameters from the expressions from **Table 3.2.**

Table 3.2: Individual heat capacity expressions for the gases involved in the process (T in K , P in atm)

$$C_{p1} = C_{H_2} = 6.952 - 4.576*10^{-4}T + 9.563*10^{-7}T^2 - 2.097*10^{-10}T^3$$

$$C_{p2} = C_{N_2} = 6.903 - 3.753*10^{-4}T + 1.93*10^{-6}T^2 - 6.861*10^{-10}T^3$$

$$C_{p3} = C_{NH_3} = 6.5846 - 6.1251*10^{-3}T + 2.3663*10^{-6}T^2 - 1.5981*10^{-9}T^3$$

$$+96.1678 - 6.7571*10^{-2}P + \left(1.687*10^{-4}P - 0.2225\right)T + (1.289*10^{-4} - 1.0095*10^{-7}P)T^2$$

$C_{p4} = C_{Inerts} = 9.70$ (mixture of 50% methane and 50% argon)

$$-\Delta H = 9184 + 7.2949T - 3.4996*10^{-3}T^2 - 3.356*10^{-7}T^3 + 1.1625*10^{-10}T^4$$

$$+6329.3 - 3.1619P - (14.3595 + 4.4552*10^{-3}P)T + (8.3395*10^{-3} + 1.928*10^{-6}P)T^2 + 51.21 - 0.14215P$$

The expressions given in Table 3.2 are valid for Temperature range of 500-900 K and pressure range of 200-1000 atm.

Enthalpy of NH_3 at 298 K (ΔH_0) is calculated using Table 3.2. ΔH_0 of NH_3 = 12600 kCal/Kgmole of NH_3.

The average molar heat capacity of the feed gas $\bar{C}_{p0}$ is constant for a given feed condition and is determined to be 7.65 kCal/Kgmole K.

$\bar{C}_{p0}$ = 7.65 kCal/Kgmole K.

ΔC is calculated considering average values of specific heats over the range 473 to 830 K. The average values are,

$C_{p1,avg}$ = 7.02 kCal/Kgmole K,

$C_{p2,avg}$ = 7.32 kCal/Kgmole K,

$C_{p3,avg}$ = 17.668 kCal/Kgmole K

Thus, ΔC = 3.29 kCal/Kgmole K.

Catalyst activity factor is assumed constant.

The maximum temperature in the catalyst bed (also called the hot spot temperature) should be below 570°C for safe operation.

Table 3.3: optimal values of parameters

Variable	Optimal values used in plant
F_1 (kg moles/hr)	2300
F_2 (kg moles/hr)	365
F_3 (kg moles/hr)	136
Y yield (kg moles/hr)	540
Catalyst activity factor	1
U (Kcal/hr m^2 ^0C)	1100
U' (Kcal/hr m^2 ^0C)	350

Ammonia mole fraction at exit of reactor is 0.23.

The dynamic model of the reactor is given in the next chapter. These equations are simplified and by using some assumptions and approximations, state space model of the reactor is developed.

Chapter – 4

RESULTS AND DISCUSSION

In this chapter, the model equations representing the synthesis converter are derived. The proposed model consists of five partial differential equations and two algebraic equations with necessary boundary and initial conditions with respect to the space and time variables, respectively.

4.1 STATE-SPACE FORMULATION OF THE AMMONIA REACTOR

4.1.1 Dynamic Model of the Reactor [13]

The dynamic model is derived under the following assumptions:

(1) No radial variation of temperature in the catalyst, cooling tube and walls.

(2) No temperature difference between the catalyst particles and the gas phase.

(3) Uniformly constant pressure throughout the converter.

(4) Negligibly small values of heat capacities of the tube walls in the reacting and heat exchanger section.

(5) No heat loss from the shell side of the heat exchanger to the environment.

(6) Absence of longitudinal diffusion of the reactants in the reactor.

(7) No transfer of enthalpy by conduction within the gas phase in the empty tube.

(8) Temperature independence of the heat capacity of the gases in the reactor only. The larger variation of temperature across the heat exchanger warrants the calculation of these parameters from the exact expressions.

(9) It is assumed that changes in flow rate, pressure and composition propagate instantaneously throughout the reactor. As a direct consequence of this assumption, this study is primarily concerned with transient analysis of the reactor for changes in the feed temperature.

All the above assumptions are proven to be valid for the tubular reactor considered (1). Under the assumptions 1 and 2 the reactor can be lumped radially into two sections as shown in the **Fig. 4.1**. The empty tube section represents the gas inside the cooling tubes, and the catalyst section include the catalyst particles and gas flowing through them.

The dynamic model equations are given below:

Material balance in the catalyst section:

$$\frac{\partial y}{\partial \alpha} = \frac{V}{F}\frac{(1+y)^2}{(1+y^*)} r(T_c, y) \qquad \text{.....4.1}$$

Energy balance in the empty tube section:

$$\frac{\partial T_T}{\partial \alpha} = \frac{US}{F\overline{C}_{p0}}(T_T - T_C) \qquad \text{.....4.2}$$

Energy balance in the catalyst:

$$\frac{-F}{h_2 s_2}(\overline{C}_{p0} - \Delta C\frac{y-y^*}{1+y})\frac{\partial T_C}{\partial \alpha} + 0.59(T_T - T_C) - \frac{F}{h_2 s_2}(\Delta H_0 - \Delta C(T_C - T_B))\frac{(1+y^*)}{(1+y)^2}\frac{\partial y}{\partial \alpha} = \frac{\partial T_C}{\partial \theta}$$

.....4.3

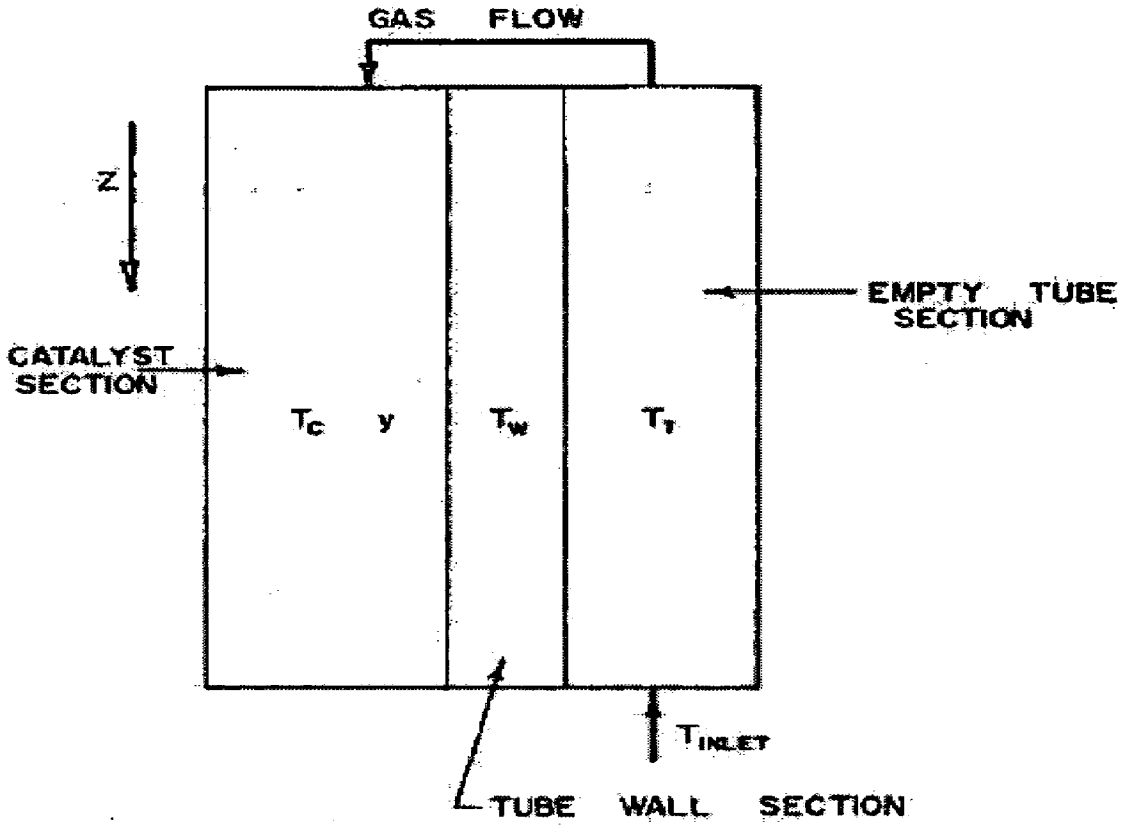

Fig. 4.1 Lumped representation of the TVA reactor (transient state) [2].

Energy balance in the shell of the heat exchanger:

$$\frac{\partial T'_s}{\partial \theta} - \left(\frac{WC_{pc}v_s}{h_2 s_2 l'}\right)\frac{\partial T'_s}{\partial \alpha'} = \left(\frac{WC_{pc}}{h_2 s_2}\right)\frac{U'S'(T'_T - T'_S)v_s}{\delta \sum_{i=1}^{4} FF_i C_{pi}} \qquad \text{.....4.4}$$

Energy balance in the tube of the heat exchanger:

$$\frac{\partial T'_T}{\partial \theta} + \left(\frac{WC_{pc}v_T}{h_2 s_2 l'}\right)\frac{\partial T'_T}{\partial \alpha'} = -\left(\frac{WC_{pc}}{h_2 s_2}\right)\frac{U'S'(T'_T - T'_S)v_T}{\sum_{i=1}^{4} n_i(\alpha', t)C_{pi}} \qquad \text{.....4.5}$$

Mixing equations and boundary conditions:

At the top of reactor-Energy balance

$$\delta(1+\beta)(T_T(\alpha=0,\theta))+\delta\beta\gamma(T_F(\theta))=(T_C(\alpha=0,\theta)) \qquad \text{.....4.6}$$

At the top of heat exchanger-Energy balance

$$\delta(T'_s(\alpha'=0,\theta))+\delta\beta(T_F(\theta))=T_T(\alpha=1,\theta) \qquad \text{.....4.7}$$

Boundary conditions:

$$\left.\begin{aligned} &y(\alpha=0,\theta)=y^*(\theta);\\ &T_C(\alpha=1,\theta)=T'_T(\alpha'=0,\theta);\\ &T'_s(\alpha'=1,\theta)=T_F(\theta); \end{aligned}\right\} \qquad \text{.....4.8}$$

The dynamic model consists of five coupled, nonlinear partial differential equations. Because of the complexity represented by this system of equations, it is not possible to obtain an analytical solution. The simplification of the dynamic model equations and simulation is done in detail.

It can be seen that even the steady state model equations have to be solved iteratively because of the boundary value nature of the problem. In the steady state case, the heat exchanger temperature at the shell entry end is matched with the feed temperature. But in the dynamic case, devising a fast converging iterative technique to match the time varying boundary conditions is a formidable task. Because of the time varying split boundary conditions associated with this problem, a convergent solution could not be obtained using hybrid simulation. Thus it became imperative to simplify the model equations so that the solution of this group of equations becomes possible within a reasonable amount of effort and computational time.

4.1.2 Linearization

In this section, the model equations (Eqs 4.1 to 4.5) are linearized around the steady state operating point corresponding to maximum yield. When the magnitudes of the disturbances are small, this linearized model adequately describes the dynamics of the reactor in the neighbourhood of the steady state operating point.

Let,

$$\left.\begin{aligned} y(\alpha,t) &= y_S + y_t \\ T_c(\alpha,t) &= T_{cS} + T_{ct} \\ T_T(\alpha,t) &= T_{TS} + T_{Tt} \\ T'_T(\alpha',t) &= T'_{TS} + T'_{Tt} \\ T'_s(\alpha',t) &= T'_{sS} + T'_{st} \end{aligned}\right\} \quad \text{.....4.9}$$

In the above equation y_s, T_{cS}, T_{TS}, T'_{TS}, and T'_{sS} represent the steady state part and y_t, T_{ct}, T_{Tt}, T'_{Tt}, T'_{st} represent the transient part of ammonia mole fraction, catalyst temperature, tube temperature in the reacting portion, tube temperature in the heat exchanger and shell temperature in the heat exchanger respectively. The steady state components are functions of α, the normalized distance.

In order to carry out the linearization we substitute Eq. (4.9) in the dynamic equations (Eqs. 4.1 to 4.5) and expand the latter around the operating point using Taylor series and neglect the higher order terms. The steady state equations which can be obtained from the dynamic model are used to further simplify these equations. During the simplification phase some terms have been neglected because their contribution is negligibly small.

Equation (4.l) can be rewritten in the form,

$$\frac{\partial y_S}{\partial \alpha} + \frac{\partial y_t}{\partial \alpha} = \frac{V}{F(1+y^*)}(1+y_S+y_t)^2[r(T_{cS}+T_{ct}, y_S+y_t)] \quad \text{.....4.10}$$

Let $\frac{V}{F(1+y^*)} = K_1$.

Expanding the right hand side of Eq. (4.10) by Taylor series and neglecting higher order terms,

$$\frac{\partial y_S}{\partial \alpha} + \frac{\partial y_t}{\partial \alpha} = K_1[(1+y_S)^2 + 2y_t(1+y_S) + y_t^2][r_S(T_{cS}, y_S) + \left.\frac{\partial r}{\partial T_c}\right|_{T_{cS}} T_{ct} + \left.\frac{\partial r}{\partial y}\right|_{y_S} y_t] \quad \text{.....4.11}$$

From steady state considerations, it is known that $\frac{\partial y_S}{\partial \alpha} = K_1(1+y_S)^2 r_S$.

Making use of this relation, and neglecting the second order terms of the perturbed values, and rearranging, we get

$$\frac{\partial y_t}{\partial \alpha} = K_1(1+y_S)^2 \left.\frac{\partial r}{\partial T_c}\right|_{T_{cS}} T_{ct} + y_t[(1+y_S)^2 \left.\frac{\partial r}{\partial y}\right|_{y_S} + 2(1+y_S)r_S + 2(1+y_S)\left.\frac{\partial r}{\partial y}\right|_{y_S}]K_1$$

..... 4.12

Similarly Eqs. (4.2) and (4.3) can be written as,

$$\frac{\partial T_t}{\partial \alpha} = K_2(T_t - T_{ct}) \quad \text{.....4.13}$$

$$-K_3\left[\overline{C}_{p0}-\Delta C\frac{y_S+y_t-y^*}{1+y_S+y_t}\right]\frac{\partial}{\partial\alpha}(T_{cS}+T_{ct})+0.59(T_{TS}+T_{Tt}-T_{cS}-T_{ct})$$

$$-K_3\left[\Delta H_0-\Delta C(T_{cS}+T_{ct}-T_B)\right]K_4\left(r_S+\left.\frac{\partial r}{\partial T_c}\right|_{T_{cS}}T_{ct}+\left.\frac{\partial r}{\partial y}\right|_{y_S}y_t\right)=\frac{\partial}{\partial\theta}(T_{cS}+T_{ct}) \quad \text{.....4.14}$$

Where,

$$K_2=\frac{US}{FC_{p0}},\quad K_3=\frac{F}{h_2S_2},\quad K_4=\frac{V}{F}$$

Making use of the corresponding steady state equation and using the following approximations,

$$\left(\overline{C}_{p0}-\Delta C\frac{y_S+y_t-y^*}{1+y_S+y_t}\right)\simeq\overline{C}_{p0}$$

$$\Delta H_0-\Delta C(Tc-TB)\simeq\Delta H_0$$

$$1+y_S+y_t\simeq1+y_S$$

Eq. 4.14 can be written as

$$-K_3\overline{C}_{p0}\frac{\partial T_{ct}}{\partial\alpha}+0.59(T_{Tt}-T_{ct})-K_3K_4\Delta H_0\left(\left.\frac{\partial r}{\partial T_c}\right|_{T_{cS}}T_{ct}+\left.\frac{\partial r}{\partial y}\right|_{y_S}y_t\right)=\frac{\partial T_{ct}}{\partial\theta} \quad \text{.....4.15}$$

Similarly Eqs. (4) and (5) can be reduced to

$$\frac{\partial T'_{st}}{\partial\theta}-K_5\frac{v_S}{l'}\frac{\partial T'_{st}}{\partial\alpha'}=\frac{K_5U'Av_S(T'_{Tt}-T'_{st})}{\delta\sum_{i=1}^{4}F_iC_{pi}} \quad \text{.....4.16}$$

$$\frac{\partial T'_{Tl}}{\partial \theta} + K_5 \frac{v_T}{l'} \frac{\partial T'_{Tl}}{\partial \alpha'} = \frac{-K_5 U' A v_T (T'_{Tl} - T'_{st})}{\sum_{i=1}^{4} n_i(\alpha', t) C_{pi}} \quad \text{.....4.17}$$

Where $K_5 = \frac{WC_{pc}}{h_2 S_2}$

The terms $\left(\frac{\partial r}{\partial T_c}\right)$ and $\left(\frac{\partial r}{\partial y}\right)$ can be obtained by differentiating r. The values of $\left(\frac{\partial r}{\partial T_c}\right)$, $\left(\frac{\partial r}{\partial y}\right)$ and r depend on steady state temperature and concentration and thus are functions of distance. From knowledge of the steady state values at various points, these terms are calculated at different points along the bed. These have been plotted in **Fig. 4.2** as functions of normalized distance. The values of these partial derivatives at different points along the reactor length are later used, to develop the lumped model.

4.1.3 Lumping Of the Linear Partial Differential Equations

In this section, we further simplify the linear distributed model of the reactor described by Eqs. (4.12)-(4.13) and (4.15)-(4.17) using discrete space approximation.

The linear partial differential equations describing the distributed model of the reactor are converted into ordinary differential equations by discretizing the length of the reactor and the heat exchanger into a number of segments. At each discretization point, the values of the quantities $\left(\frac{\partial r}{\partial T_c}\right)$, $\left(\frac{\partial r}{\partial y}\right)$ and r_S appearing in Eqs. (4.12) and (4.15) are obtained from **Fig. 4.2** by computing the weighted

average over the interval. The accuracy of the lumped model obviously depends on the number of discretization steps used. The larger the number of intervals, the better is the accuracy. Also the number of differential equations increases linearly with the number of intervals chosen.

On the other hand, coarser discretization may lead to inaccurate models. In this study we consider the effect of the fineness of discretization and conclude that the reacting portion can be divided into five parts and the heat exchanger into two parts as shown in **Fig. 4.3.** The results of this study can be found in the later sections. **Orcutt & Lamb** have used the linearized lumped model to investigate the stability of the ammonia reactor. They also have concluded that the reactor dynamics for this purpose can be satisfactorily described by dividing the reacting section into five parts and treating the heat exchanger as a single unit. In what follows, the discretization procedure is presented.

Equation (4.12) can be arranged as,

$$\frac{\partial y_t}{\partial \alpha} = a(\alpha) y_t + b(\alpha) T_{ct} \qquad \text{.....4.18}$$

where

$$a(\alpha) = \left[(1+y_S)^2 \left.\frac{\partial r}{\partial y}\right|_{y_S} + 2(1+y_S) r_S + 2(1+y_S) \left.\frac{\partial r}{\partial y}\right|_{y_S} \right] K_1 \qquad \text{.....4.19}$$

and

$$b(\alpha) = K_1 (1+y_S)^2 \left.\frac{\partial r}{\partial T_c}\right|_{T_{cS}} \qquad \text{.....4.20}$$

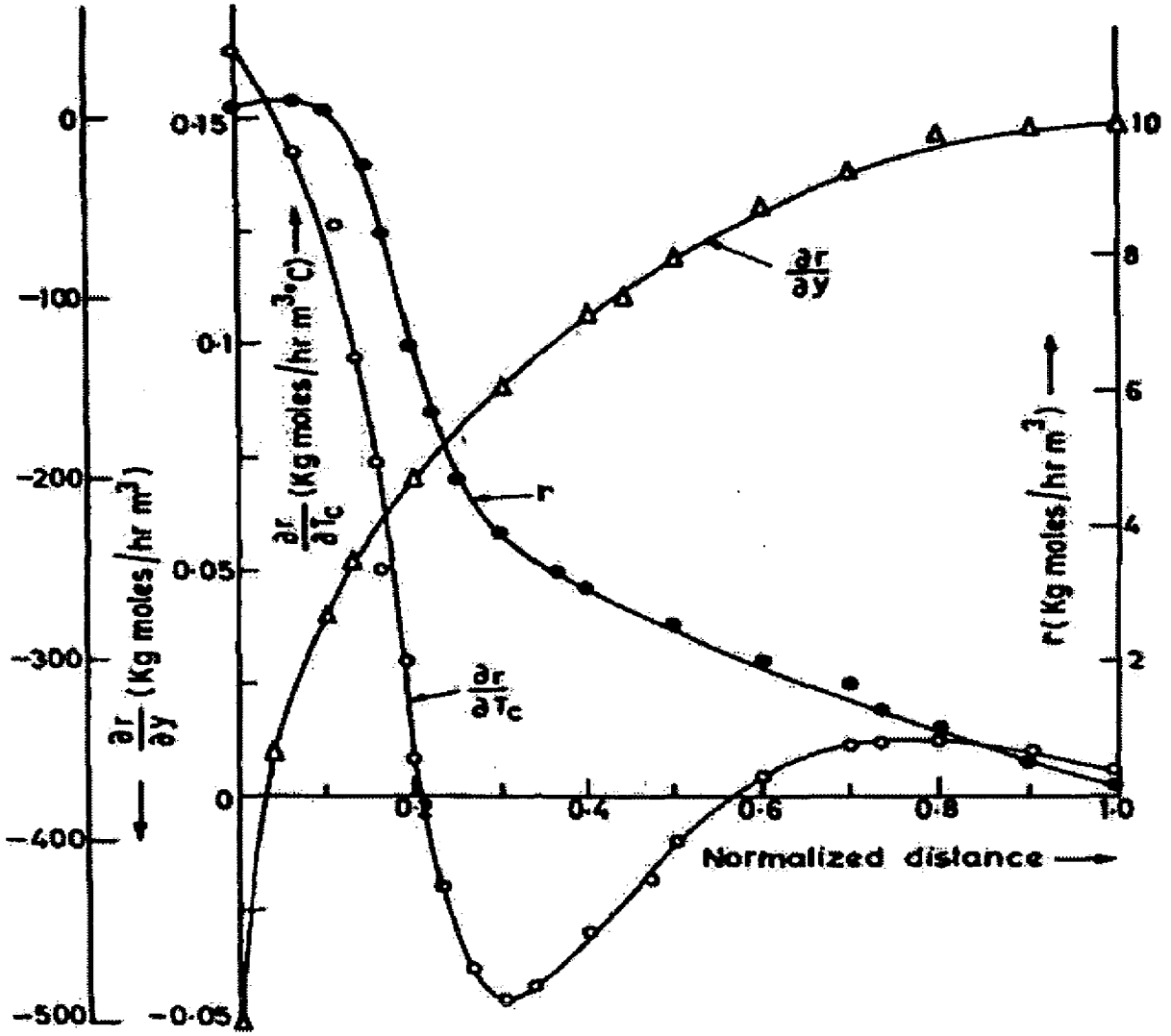

Fig. 4.2 Variation of $\left(\frac{\partial r}{\partial T_c}\right)$, $\left(\frac{\partial r}{\partial y}\right)$ and r with normalized distance [15].

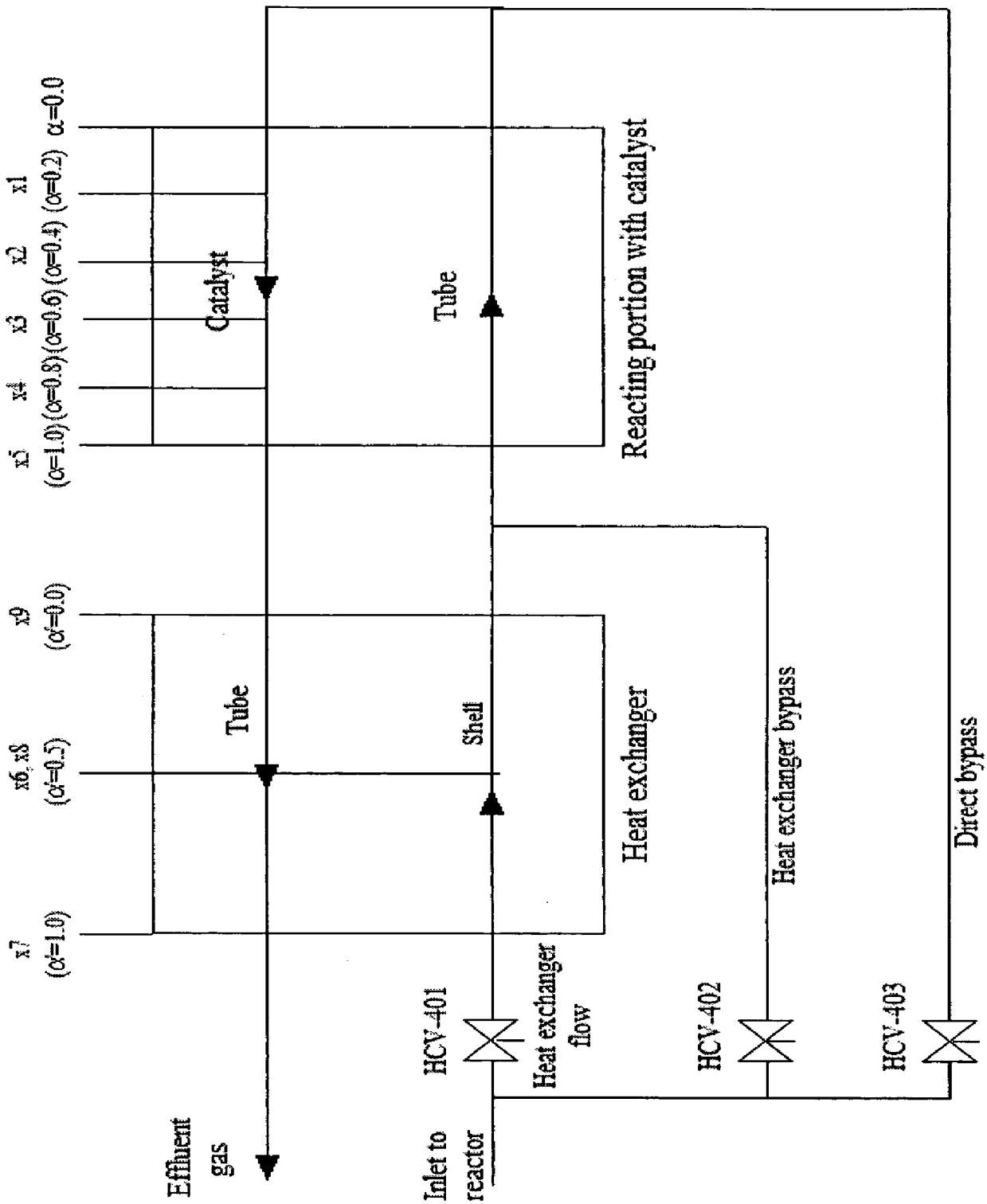

Fig. 4.3 Schematic diagram of the ammonia reactor after discretization [13]

Substituting

$$\left.\frac{\partial y_t}{\partial \alpha}\right|_j = \frac{y_t(j) - y_t(j-1)}{\Delta\alpha}$$

into Eq. (4.18) and simplifying we get

$$y_t(j)\left[\frac{1}{\Delta\alpha} - a(j)\right] = \frac{y_t(j-1)}{\Delta\alpha} + b(j)T_{ct}(j) \qquad \text{.....4.21}$$

here j = 1, 2, 3 ...N

where $\Delta\alpha$ is the step size of normalized distance.

The above equation can be compactly written as

$$Ay = Bt_c + dy_0 \qquad \text{.....4.22}$$

where y and t_c are the N x 1 vectors representing the perturbed values of ammonia mole fraction and catalyst temperature at different points, **A** and **B** are N x N matrices, ***d*** is N x 1 vector and $y_0 = y_t(0)$.

Similarly Eq. (4.14) can be written as,

$$Ht_t = dt_{t0} - K_2 t_c \qquad \text{.....4.23}$$

H is an N x N matrix, t_t is an N x 1 vector representing the perturbed values of tube temperature at different points and $t_{t0} = T_t(0)$. Substituting the values of various constants in Eq. (4.15) we obtain

$$0.59T_{Tt}(j) + T_{ct}(j)\left[c(j) - \frac{0.506}{\Delta\alpha}\right] + \frac{0.506}{\Delta\alpha}T_{ct}(j-1) + d(j)y_t(j) = \frac{dT_{ct}(j)}{d\theta} \qquad \text{.....4.24}$$

where,

$$c(j) = -0.59 - K_4 K_5 \Delta H_0 \left.\frac{\partial r}{\partial T_c}\right|_{T_{cs}}$$

$$d(j) = -\left.\frac{\partial r}{\partial y}\right|_{yS} K_4 K_5 \Delta H_0$$

Equation (4.16) can be written as,

$$\dot{t}_c = Ct_c + Dy + 0.59t_t + 0.506dt_{c0} \qquad \text{where } t_{c0} = T_{ct}(0). \qquad \text{.....4.25}$$

Solving Eqs. (4.22) and (4.23) for y and t_t and substituting these into Eq (4.25) we get

$$\dot{t}_c = \left[C + DA^{-1}B - 0.59 * 3.1888H^{-1}\right]t_c + \left[DA^{-1}d \quad 0.506d \quad 0.59H^{-1}d\right]\begin{bmatrix} y_0 \\ t_{c0} \\ t_0 \end{bmatrix}$$

.....4.26

Next let us consider Eqs. (4.16) and (4.17). Representing t'_s and t'_t as the perturbed values of shell side and tube side temperatures in the heat exchanger and substituting the values of various constants, we obtain

$$\frac{\partial t'_s}{\partial \theta} - 9.4\frac{\partial t'_s}{\partial \alpha} = 12.8\left(t'_t - t'_s\right) \qquad \text{.....4.27}$$

$$\frac{\partial t'_t}{\partial \theta} + 47\frac{\partial t'_t}{\partial \alpha} = 53.2\left(t'_s - t'_t\right) \qquad \text{.....4.28}$$

In arriving at the linear Eq. (4.28) from (4.17), the denominator of the latter equation has been obtained by taking the average of the steady state values of this term at various points in the heat exchanger. Since the heat exchanger is divided into two parts, Eqs. (4.27) and (4.28) can be written as

$$\frac{dt'_s(j)}{d\theta} = 12.8t'_t(j) - 31.6t'_s(j) + 18.8t'_t(j+1) \qquad \text{where j = 0, 1} \qquad \text{.....4.29}$$

$$\frac{dt'_t(j)}{d\theta} = 53.2t'_s(j) - 147.2t'_t(j) + 94t'_t(j-1) \qquad \text{where j = 1, 2} \qquad \text{.....4.30}$$

The boundary conditions are, $t'_s(2) = t_f =$ perturbation in feed temperature and $t'_t(0) = t_c(\alpha = 1)$.

The mixing equation at the top of the reactor, Eq (4.6), can be perturbed around the steady state to yield

$$t_{c0} = 0.955t_{t0} + 0.047t_f - 0.0595u_3 + 0.0029u_1 + 0.0029u_2 \qquad \text{.....4.31}$$

where u_1, u_2 and u_3 are the perturbations in $F_1 - F_3$.

Equation (4.7) representing the mixing equation at the top of the heat exchanger can be linearized to result in

$$t_t(5) = 0.00288u_1 - 0.019u_2 + 0.87t'_s(0) + 0.131t_f \qquad \text{.....4.32}$$

By repeated application of Eq. (4.13) in a backward difference scheme to obtain an expression for t_{t0} and by using this expression along with Eqs. (4.31-4.32) we get a set of five coupled differential equations from Eq. (4.26). Similarly one can get a set of four coupled differential equations from Eqs. (4.29-4.30). The first set of five linear ordinary differential equations represent the dynamics of the reacting portion whereas the latter set of 4 equations represent the dynamics of the heat

exchanger. If these nine temperatures form the elements of a state vector then one can obtain the state variable form of the dynamic equations which is presented in the following section.

4.1.4 State Space Representation

Let

$$x^T \triangleq [x_1, x_2, x_3, x_4, x_5, x_6, x_7, x_8, x_9]$$

$$= [t_c(1), t_c(2), t_c(3), t_c(4), t_c(5), t'_t(1), t'_t(2), t'_s(0), t'_s(1)]$$

$$u^T \triangleq [u_1, u_2, u_3]$$

$$d^T \triangleq [t_f, y_0]$$

$t_c(1), t_c(2), t_c(3), t_c(4)$ and $t_c(5)$ are incremental catalyst temperatures at the five discrete points in the reactor. Then the linearized equations (4.26) and (4.29)-(4.30) after minor arrangements can be represented by

$$\dot{x}(t) = Ax(t) + Bu(t) + Dd(t) \qquad \text{.....4.33}$$

where **x**(t) is a 9 x 1 state vector, **u**(t) is a 3 x 1 manipulated vector, **d**(t) is a 2 x 1 disturbance vector and **A**, **B** and **D** are 9 x 9, 9 x 3 and 9 x 2 matrices respectively.

$$A = \begin{bmatrix} -4.019 & 5.12 & 0 & 0 & -2.082 & 0 & 0 & 0 & 0.87 \\ -0.346 & 0.986 & 0 & 0 & -2.34 & 0 & 0 & 0 & 0.97 \\ -7.909 & 15.407 & -4.069 & 0 & -6.45 & 0 & 0 & 0 & 2.68 \\ -21.816 & 35.606 & -0.339 & -3.87 & -17.8 & 0 & 0 & 0 & 7.39 \\ -60.196 & 98.188 & -7.907 & 0.340 & -53.008 & 0 & 0 & 0 & 20.4 \\ 0 & 0 & 0 & 0 & 94 & -147.2 & 0 & 53.2 & 0 \\ 0 & 0 & 0 & 0 & 0 & 94 & -147.2 & 0 & 0 \\ 0 & 0 & 0 & 0 & 0 & 12.8 & 0 & -31.6 & 0 \\ 0 & 0 & 0 & 0 & 12.8 & 0 & 0 & 18.8 & -31.6 \end{bmatrix}$$

$$B = \begin{bmatrix} 0.01 & -0.011 & -0.051 \\ 0.003 & -0.021 & 0 \\ 0.009 & -0.059 & 0 \\ 0.024 & -0.162 & 0 \\ 0.068 & -0.445 & 0 \\ 0 & 0 & 0 \\ 0 & 0 & 0 \\ 0 & 0 & 0 \\ 0 & 0 & 0 \end{bmatrix} \qquad D = \begin{bmatrix} 0.251 & -1438.916 \\ 0.147 & -323.846 \\ 0.405 & -82.771 \\ 1.13 & -22.637 \\ 3.07 & -5.456 \\ 53.2 & 0 \\ 18.8 & 0 \\ 0 & 0 \\ 0 & 0 \end{bmatrix}$$

4.1.5 Stability of State-Space Models

A state-space model is said to be stable if the response *x(t)* is bounded for all *u(t)* and *d(t)* that are bounded. The stability characteristics of a state-space model can be determined from a necessary and sufficient condition:

Stability Criterion for State-Space Models:

> A state-space model (Eq. 4.33) will exhibit a bounded response *x(t)* for all bounded *u(t)* and *d(t)*, if and only if all of the eigen values of **A** have negative real parts.

Note that stability is solely determined by **A**; the elements of **B** and **C** have no effect.

The stability of Eq. 4.33 is therefore determined by finding the eigen values of **A.**

Here eigen values are calculated using the **MATLAB** command, ***eig***, after defining **A**:

The eigen values of **A** are:

-147.20, -153.1, -50.65, -38.76, -14.38, -4.52, -4.56, -3.86 and -4.54.

Because all the nine eigen values have negative real parts, the state space model is stable.

4.2 SIMULATED RESPONSES

The nine ordinary differential equations given by Eq. (4.33) are simulated using C++ program using Runge-Kutta 4th order method.

The purpose of this simulation study is

1. to check whether the response obtained using the linear model equation agrees with those reported in the literature [2].
2. to determine the effect of the fineness of discretization on the response and from these results to fix the discretization intervals for both the reactor and heat exchanger.
3. apart from the above reasons, the knowledge of the open-loop behaviour of the system is important in determining the specifications for proceeding with the control system design.

The system is subjected to a step disturbance of 5°C in the feed temperature which has a steady state value of 42°C. This corresponds to a 12.5% perturbation after this nominal value. Even though feed temperature and ammonia mole fraction are the components of the disturbance vector, we consider the former because the results obtained can be compared with those reported in the literature. Moreover, the effect of thermal perturbations are of interest to the plant operators. The response at different points along the length of the reactor is shown in **Fig. 4.4.** The steady state program is run with the new feed temperature (the nominal feed

temperature incremented by the step disturbance). The perturbed temperature profile thus obtained should check with the profile obtained by the dynamic simulation. It has been established that the profiles match within reasonable accuracy. The error in the steady state temperature at the exit of the catalyst bed is 0.4%. In the absence of experimental data, the results obtained are compared with those reported by Brian et al. [2]. The trend of the response agrees with that shown in their work.

The pulse response of the system at the reactor exit is shown in **Fig. 4.5**. The initial "inverse response' is clearly reflected in both the above response curves.

In order to gain a greater insight into plant dynamics, the system is subjected to a step change of 7.5 kgmoles/hr in direct bypass flow rate. The response curves are shown in **Fig. 4.6**. It is interesting to note that the "inverse response" is more pronounced as the bottom end of the reactor is approached.

4.3. EFFECT OF FINENESS OF DISCRETIZATION

In an earlier section the linear state space model is derived after dividing the reacting section into 5 parts and heat exchanger into 2 parts. The division of the heat exchanger into 2 equal parts is justified because its dynamics is very fast and this is not as significant as the reacting portion where the main reaction takes place. The partial derivatives being functions of the length of the reactor, weighted average values of these are used in the model.

To study the sensitivity of the dynamic model of the system to the number of discretization steps, the reacting section is considered separately. The state variable representation for this is obtained for different cases of discretization: N = 3, 4, 5

and 7, where N is the number of steps into which the reactor is divided. The reactor shows unstable behaviour when $N \leq 3$ even though this corresponds to a stable operating point.

The dynamic behaviour of the reactor for N = 4, 5 and 7 is considered. The criterion used for comparing these cases is the percentage error in the steady state temperature at the exit of the catalyst bed. This information is summarized in Table 4.1. From this table, it is clear that no significant improvement can be achieved by choosing $N > 5$ thus justifying our earlier choice of five discretization intervals for the reactor length.

Table 4.1: Percentage error in catalyst bed exit temperature for different discretization step sizes

N	Percentage error in $t_c(5)$
3	Reactor is unstable
4	0.6%
5	0.4%
7	0.32%

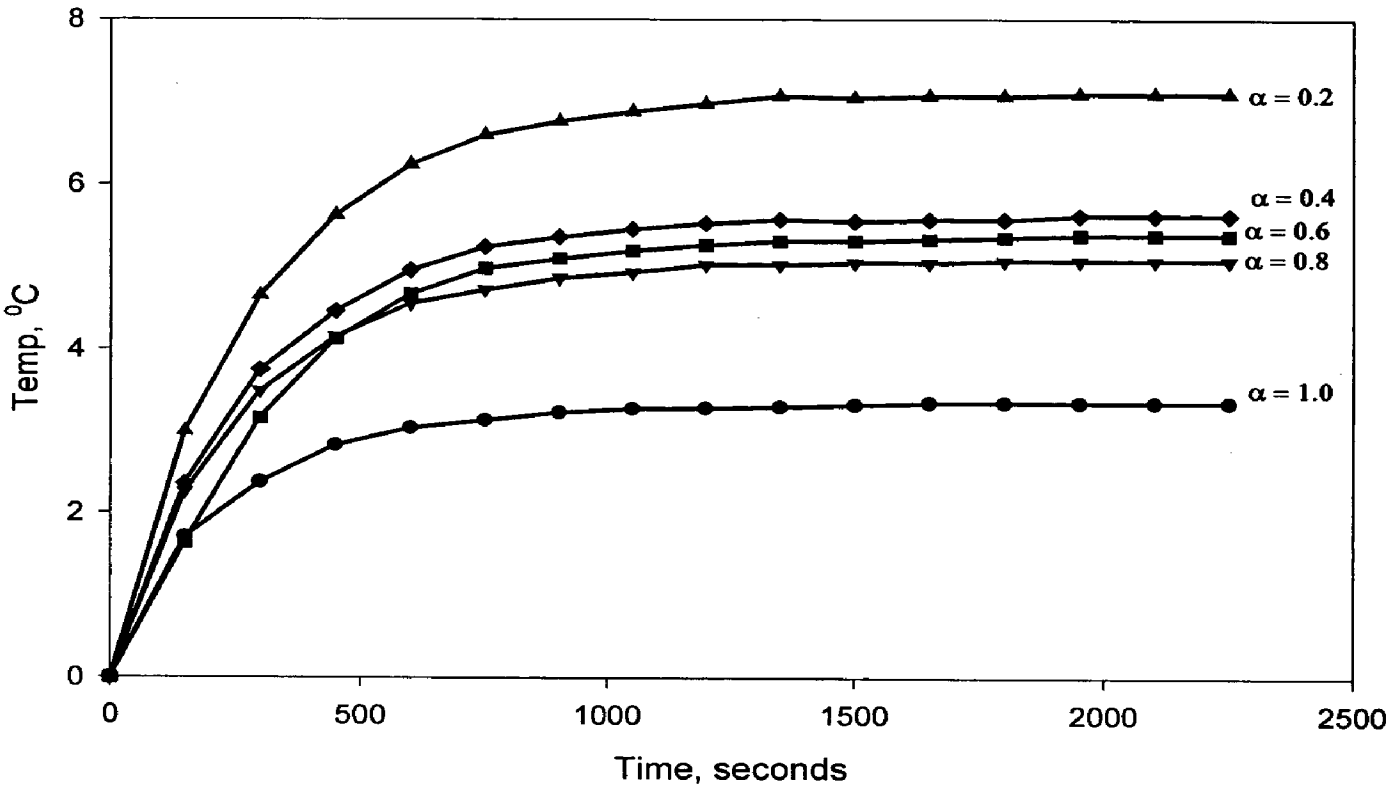

Fig. 4.4 Open-loop response to 5^0C step in feed temperature (N = 5).

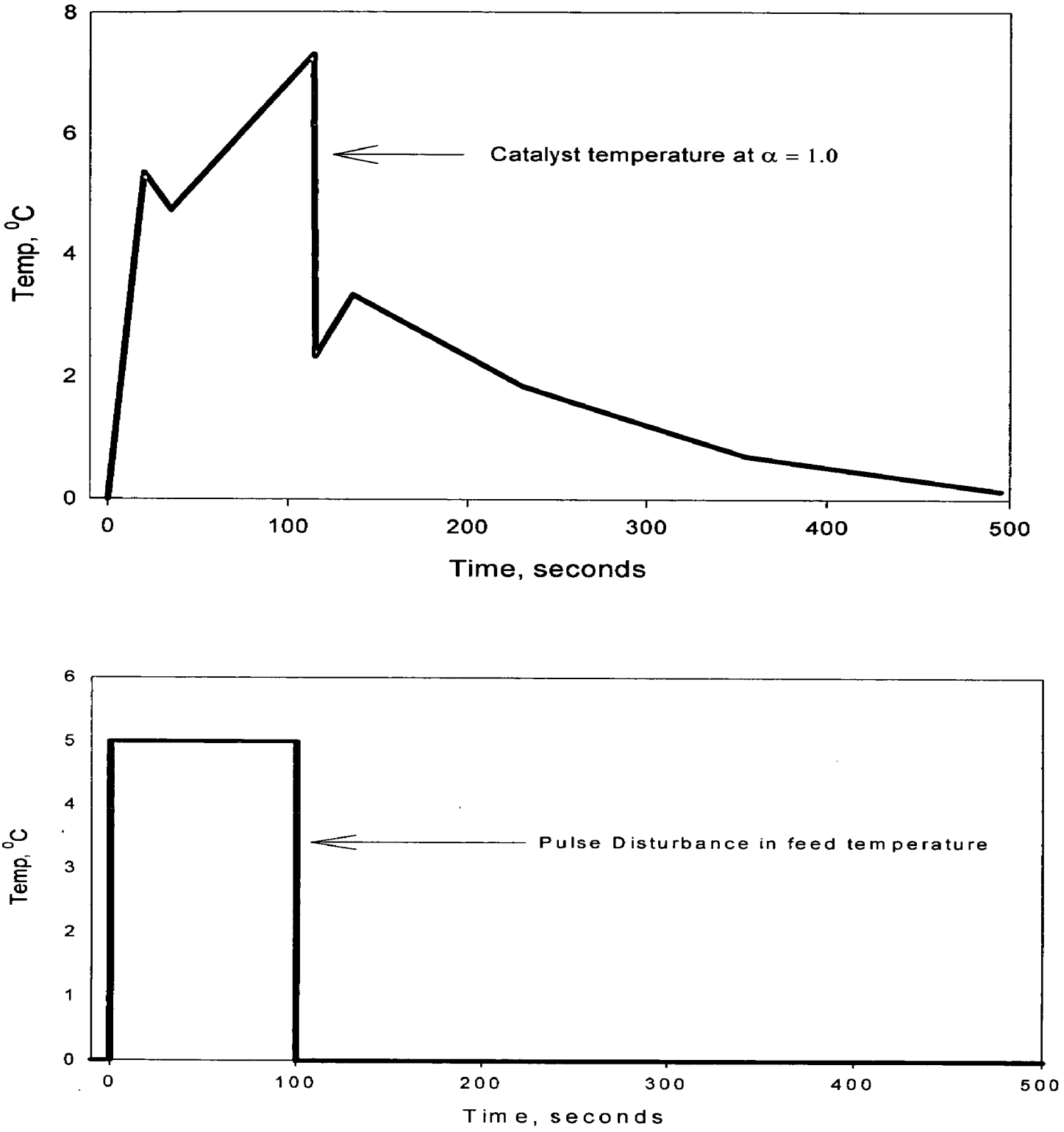

Fig. 4.5 Pulse response at catalyst bed exit end.

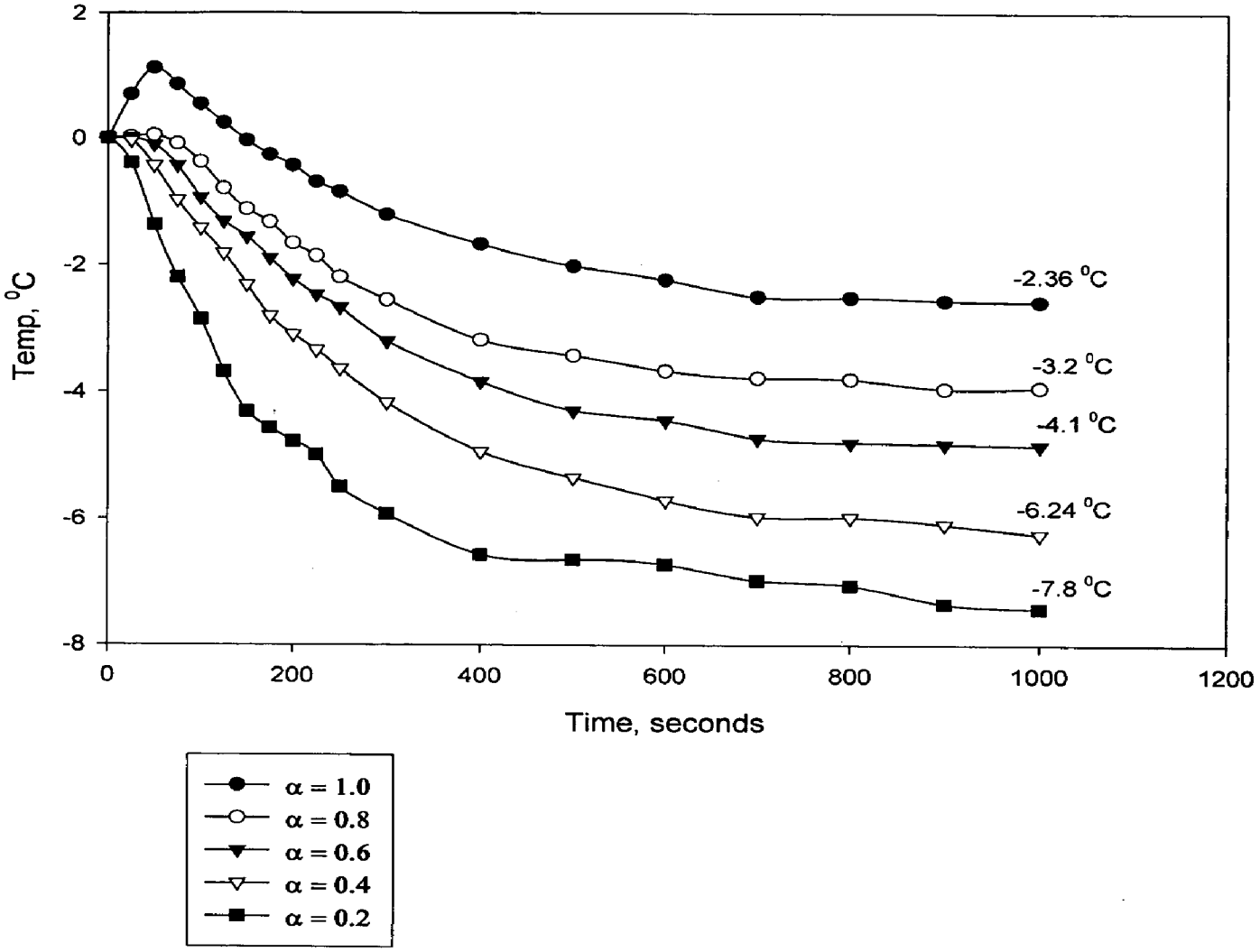

Fig. 4.6 Response to step change in direct bypass flow rate (step: 7.5 kg moles/hr).

4.4 PID CONTROL FOR THE REACTOR

In an earlier paper by Patnaik et al. [14], the authors have developed an optimization program to determine the optimum temperature profile that maximizes the ammonia yield. The reactor is to be operated at the "blow-out" point (highest temperature stable operating point) to achieve higher throughput. However, the feed concentration and temperature disturbances tend to change the temperature profile inside the reactor and thus drive the reactor away from this maximal yield operating point. Hence, regulation of the temperature along the length of the reactor around the optimal profile in the presence of disturbance inputs is important and forms a dominant design objective for control system design.

The model has three control inputs (flow rates), two disturbance inputs (concentration and temperature variables), and nine state variables (temperatures).

It is observed that the direct bypass flow rate has the maximum influence on the temperature profile of the reactor. The other two flow rates remain at their steady-state optimal values. In designing the control law, we consider the following discrete equivalent of the continuous **PID** controller employing a rectangular integration scheme:

$$p_n = \bar{p} + K_c\left[e_n + \frac{T}{T_I}\sum_{k=0}^{n} e_k + \frac{T_D}{T}(e_n - e_{n-1})\right] \qquad \text{.....4.34}$$

T = the sampling period (the time between successive measurement of the controlled variable).

e_n = error at the nth sampling instant for n = 1, 2, 3, ...

p_n = controller output at the nth sampling instant

K_c = Controller Gain

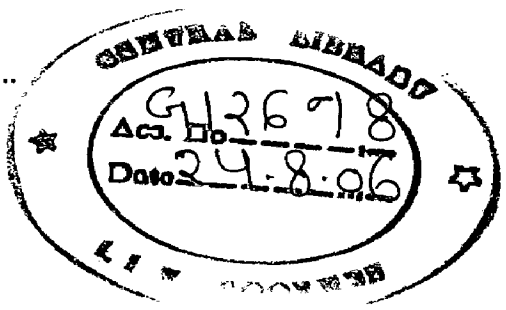

The parameters K_c, T_I and T_D in **(4.34)** need to be tuned to obtain the desired response. Controller gains obtained using the root locus method are chosen as initial values and later tuned to get acceptable responses.

In this, temperature (T) inside the reactor is controlled.

Manipulated variable used is direct bypass flow rate, q_3.

Disturbance variable is inlet temperature of component A, T_{in}.

The block diagram of the reactor temperature control is given in **Fig. 4.7**

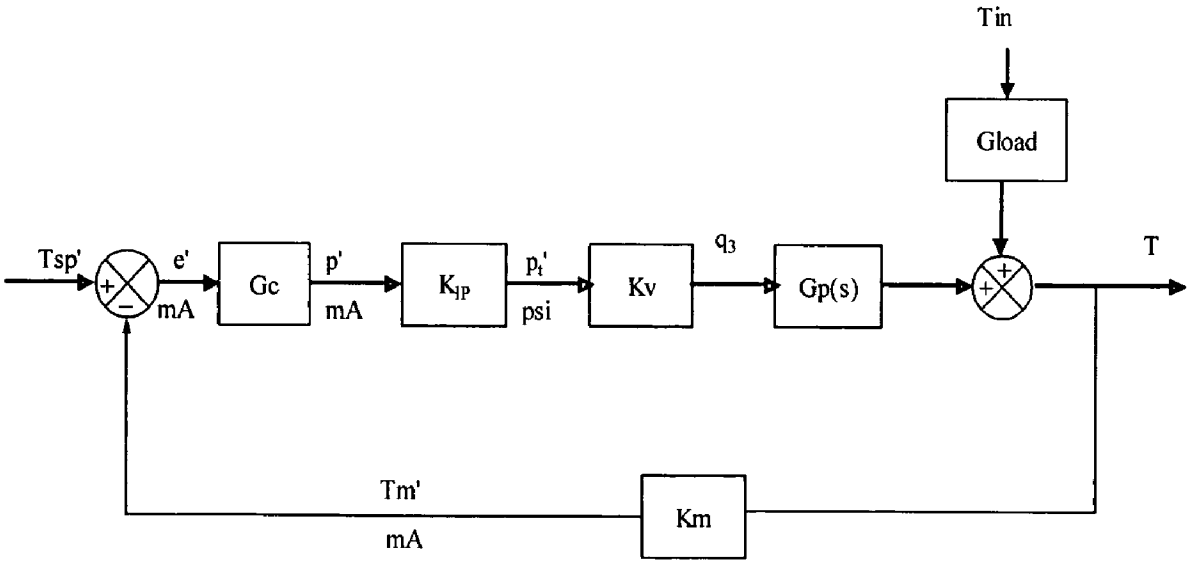

Fig 4.7 Block diagram for the reactor temperature control

Each of the variables inside the block diagrams should be known to get the response.

Measuring element chosen is T-type thermocouple which has a time constant of 3 millisec and temperature range of 350 K to 750 K.

$$Km = \frac{\text{(output range)}}{\text{(input range)}} = \frac{(100 - 0)\%}{(450\text{-}350)} = 1\ \%/K$$

The control gain Kv must include the I/P transducer gain in order to provide a steady-state relation between the computer output p (in %) and the flow rate through the control valve, q_3.

$$Kv = K_{IP}\frac{dq_3}{dp_t} \qquad \text{..... (4.35)}$$

where p_t is the transducer output pressure.

$K_{IP} = (15\text{-}3)/(20\text{-}4) = 0.75$ psig/mA

Eq (4.35) can be written as

$$Kv = K_{IP}(\frac{dq_3}{dl}).(\frac{dl}{dp_t}) \qquad \text{..... (4.36)}$$

If valve actuator is designed so that the fraction of lift l varies linearly with the IP transducer output p_t, then

$$\frac{dl}{dp_t} = \frac{\Delta l}{\Delta p_t} = \frac{1-0}{15-3} = .0833 psig^{-1}$$

Let equal percentage valve is used.

Design equation for sizing control valves is given by,

$$q = C_v f(l)\sqrt{\frac{\Delta P}{g_s}} \qquad \text{.....4.37}$$

Where q = flow rate f(l) = flow characteristic

l = valve lift Cv = valve coefficient

ΔP = pressure drop across the valve

g_s = specific gravity of the fluid.

Specification of the valve size is dependent on the so-called *valve characteristic* **f.** Three control valve characteristics are mainly used. For a fixed pressure drop across the valve, the flow characteristic $f(0 \le f \le 1)$ is related to the lift $l(0 \le l \le 1)$, that is, the extent of valve opening, by one of the following relations:

$$\begin{aligned} &\text{Linear} && : && f = l \\ &\text{Quick opening} && : && f = \sqrt{l} \qquad \text{..... 4.38} \\ &\text{Equal percentage} && : && f = R^{l-1} \end{aligned}$$

where R is a valve design parameter that is usually in the range 20 to 50. The quick-opening valve above is referred to as a *square root valve.* The equal percentage valve is given that name because the slope of the f vs. l curve, df/dl, is proportional to f, leading to an equal percentage change in flow for a particular change in l anywhere in the range.

One widely used guideline is that the valve be half open at nominal operating conditions.

Let equal percentage valve is used with **R** = 35.

Then valve design equation can be expressed as (from Eqs 4.37 and 4.38)

$$q_3 = Z(35)^{l-1} \qquad \text{..... 4.39}$$

where $Cv\sqrt{\Delta Pv} = Z$

We know that valve is half opened at nominal conditions. Value of q_3 at nominal condition is given in **Table 3.1** which is 3000 m^3/hr.

Hence at l = 0.5, q_3 = 3000 m^3/hr.

Substituting in Eq. 4.39 we get Z = 17751

Hence $q_3 = 17751(35)^{l-1}$.

By finding (dq_3/dl) at nominal conditions and substituting it in Eq. 4.36 we get the value of Kv. Kv is found to be 385.83.

$$Kv = 385.83$$

Using the above mentioned steps, numerical integration of the differential equation by using C++ program, we can solve the block diagram (**Fig. 4.6**) for different values of normalized distance.

The graphical results obtained are given in **Fig. 4.8.**

The graph for $\alpha = 1.0$ is given separately because it does not have any offset.

It is observed from simulation studies that the PID controller at the exit end of the reacting portion has a slow speed of response (220 s) and results in a maximum temperature change of 200 percent (expressed as a percentage of input disturbance of 5^oC). The choice of sampling time is an important aspect in the design of all discrete control algorithms since it can be regarded as one of the critical control parameters. Since the temperature variables under consideration have relatively slow dynamics, a choice of 30 s for the sampling time has proven quite reasonable. The other parameters used are Kc = 2.0, T_D = 40 secs and T_I = 10 secs.

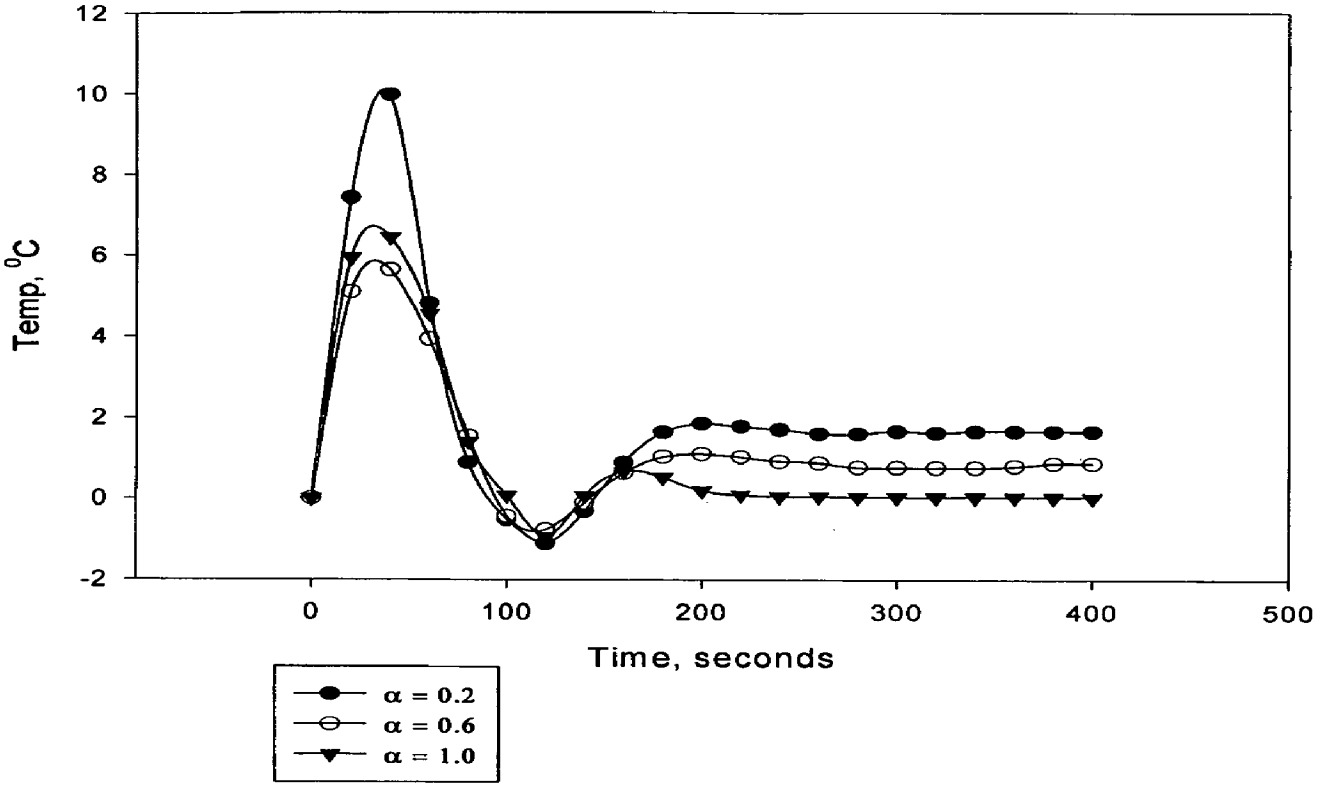

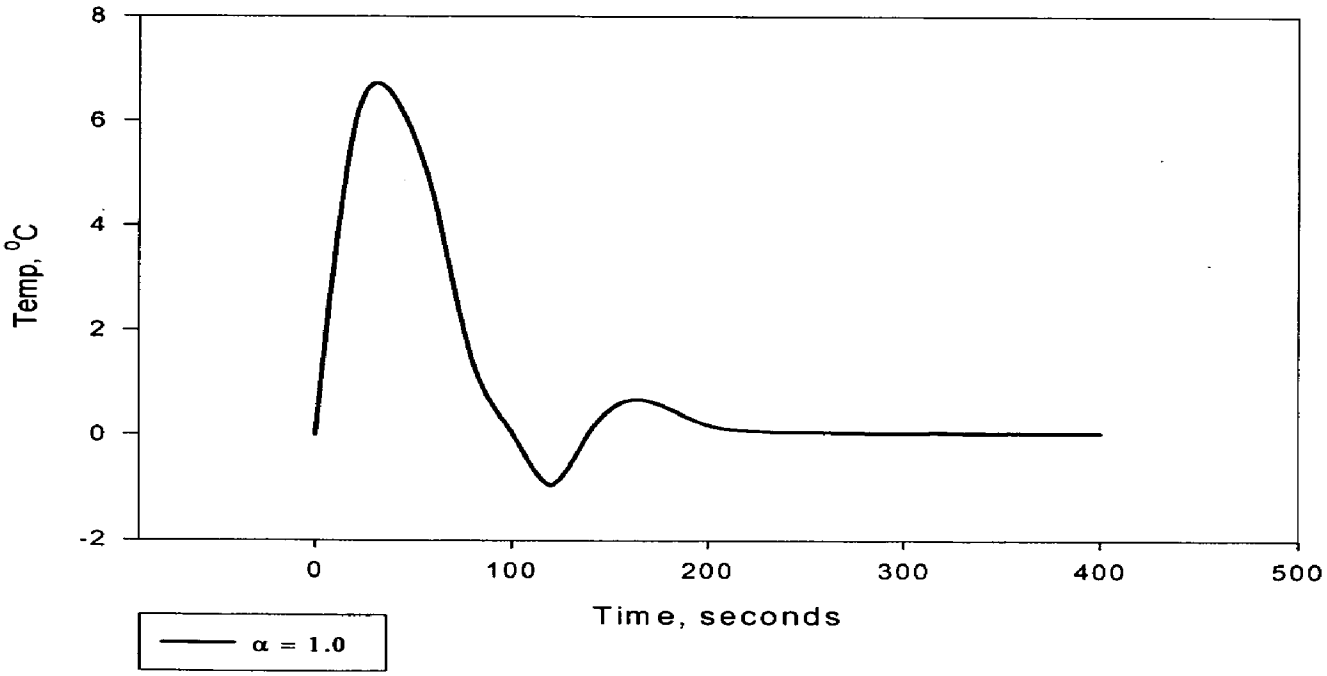

Fig 4.8 Response with a discrete PID controller

CHAPTER 5

CONCLUSIONS

Most of the chemical processes are nonlinear. The importance of nonlinear models and approximating these models has been studied here. It has also been discussed about different types of block-oriented models and their representation.

There are many nonlinear modeling methods. Depending on the system, different approaches exist to propose models for nonlinear dynamic systems. Since no model structure can cover all possible nonlinear systems, approximations will be introduced.

The problem considered is the control of an ammonia reactor. Economic gains for such reactors accrue from the choice of process conditions that result in the operation of the reactor at maximum yield steady state operating point and by improved control which allows smaller excursions and faster responses to set point changes and faster responses and less variation in product yields to load disturbances.

The ability to track and operate at the optimal operating point requires the combination of good process models, accurate identification of its parameters and appropriately chosen control system structure. For chemical reactors, essential parameters to be estimated include kinetic reaction rate constants as well as poisoning and fouling and the control objective is to maintain its temperature profile close to the optimal one.

Accordingly, this study laid emphasis on development of dynamic models. The dynamic model of the ammonia reactor consists of five partial differential equations and two algebraic equations with necessary boundary and initial

conditions with respect to the space and time variables, respectively. It is simplified and its state-space model is developed by using some assumptions and approximations which are of proven validity in actual operation. The required data is taken from the cited reference.

The state-space model is used to develop the open loop response of the reactor for a step change of 5^0C in feed temperature along the length of the reactor. The pulse response of the system at the reactor exit is developed. In order to gain a greater insight into plant dynamics, the system is subjected to a step change in direct bypass flow rate.

Then the reactor temperature is controlled using PID controller. The response of the reactor temperature along the length of the reactor is also shown.

A logical next step would be to extend these results to include the front end of the ammonia process.

BIBLIOGRAPHY

1. **Baddour R F, Brian P L T, Logeais B A and Eymery T P** (1965)
   Steady-state simulation of an ammonia synthesis converter
   Chemical Engineering Science 20, pp. 281-292.

2. **Brian P L T, Baddour R F, and Eymery T P** (1965)
   Transient behaviour of an ammonia synthesis reactor
   Chemical Engineering Science 20, pp. 297-310.

3. **Crama, ftp://eleftp.vub.ac.be/Papers/PhCRAMA/book.pdf.**

4. **Dongmei Zhai, Derrick K. Rollins Sr., Nidhi Bhandari, Huaiqing Wu** (April 2006)
   Continuous-time Hammerstein and Wiener modeling under second-order static nonlinearity for periodic process signals
   Computers and Chemical Engineering.

5. **Ender L and R Macel Filho** (2000)
   Design of Multivariable Controller Based On Neural Networks
   Computers and Chemical Engineering 24, pp. 937-943.

6. **Federico Zardi and Dominique Bonvin** (1992)
   Modeling, Simulation and Model Validation for an Axial-Radial Ammonia Synthesis Reactor
   Chemical Engineering Science, Vol. 47, No. 9-11, pp. 2523-2528.

7. **Juan C. Gomez and Enrique Baeyens** (2004)
Identification of block-oriented nonlinear systems using orthonormal bases
Journal of Process Control 14, pp. 685–697.

8. **Kenneth R. Harris, Ahmet Palazoglu** (2003)
Control of nonlinear processes using functional expansion models
Computers and Chemical Engineering 27, pp. 1061-1077.

9. **Lusson Cervantes A, Agamennoni O E and Figueroa J L** (2003)
Use of Weiner Nonlinear MPC Method to Control a CSTR with Multiple Steady State
Latin American Applied Research 33, pp. 149-154.

10. **Menold P H and Allgower F** (1997)
Nonlinear Structure Identification of Chemical Processes
Computers and Chemical Engineering, Vol. 21, pp. S137-S142.

11. **Mulholland. M** (1988)
Application of Minimum-Variance Control Strategies On An Ammonia Plant
Computers and Chemical Engineering, Vol. 12, No. 4, pp. 297-302.

12. **Nidhi Bhandari and Derrick K. Rollins** (2003)
Continuous-Time Multiple-Input, Multiple-Output Weiner Modeling Method
Ind. Eng. Chem. Res. 42, pp. 5583-5595.

13. **Patnaik L M, Sarma I G and Viswanadham N** (August 1980)
Computer Control Algorithms for a Tubular Ammonia Reactor
IEEE Transactions on Automatic Control, Vol. AC-25, No. 4, pp. 642.

14. **Patnaik L M, Sarma I G and Viswanadham N** (May 1979)
Design of single variable controllers for ammonia reactors
Chemical Engineering Science 35, pp. 754

15. **Patnaik L M, Sarma I G and Viswanadham N** (May 1980)
State Space Formulation of Ammonia Reactor Dynamics
Computers and Chemical Engineering 4, pp. 215-222.

16. **Pearson R.K and Pottman M** (2000)
Gray-box identification of block-oriented nonlinear models
Journal of Process Control 10, pp. 301.

17. **Philippe Crama, Johan Schoukens** (2004)
Hammerstein-Weiner system estimator initialization
Automatica 40, pp. 1543-1550.

18. **Rohit S. Patwardhan, Lakshminarayanan S, and Sirish L. Shah** (July 1998)
Constrained Nonlinear MPC Using Hammerstein and Weiner Models
AICHE Journal 44(7), pp. 1611-1622.

19. **Yost C C, Yurtis C R and Ryskamp C J** (April 1980)
Advanced Control at Wycon's Ammonia Plant
AICHE, pp. 31.

20. **Yucai Zhu** (2002)
Estimation of N-L-N Hammerstein-Weiner model
Automatica 38, pp. 1607-1614.